



Published in final edited form as:

Behav Brain Res. 2013 February 1; 238: 211–226. doi:10.1016/j.bbr.2012.10.026.

Memory in aged mice is rescued by enhanced expression of the GluN2B subunit of the NMDA receptor

B. L. Brim^{a,b,c}, R. Haskell^d, R. Awedikian^e, N.M. Ellinwood^e, L. Jin^{a,b}, A. Kumar^f, T.C. Foster^f, and K. Magnusson^{a,b,c,*}

^aMolecular and Cellular Biosciences Program, Oregon State University, Corvallis, OR, 97331, U.S.A

^bDepartment of Biomedical Sciences, College of Veterinary Medicine, Oregon State University, Corvallis, OR, 97331, U.S.A

^cHealthy Aging Program, Linus Pauling Institute, Oregon State University, Corvallis, OR; 97331, U.S.A

^dViraQuest, Inc., North Liberty, IA; 52317, U.S.A

^eDepartment of Animal Sciences, Iowa State University, Ames, IA, 50011, U.S.A

^fDepartment of Neuroscience, McKnight Brain Institute, University of Florida, Gainesville, FL, 32611, U.S.A

Abstract

The GluN2B subunit of the *N*-methyl-D-aspartate (NMDA) receptor shows age-related declines in expression across the frontal cortex and hippocampus. This decline is strongly correlated to age-related memory declines. This study was designed to determine if increasing GluN2B subunit expression in the frontal lobe or hippocampus would improve memory in aged mice. Mice were injected bilaterally with either the GluN2B vector, containing cDNA specific for the GluN2B subunit and enhanced Green Fluorescent Protein (eGFP); a control vector or vehicle. Spatial memory, cognitive flexibility, and associative memory were assessed using the Morris water maze. Aged mice, with increased GluN2B subunit expression, exhibited improved long-term spatial memory, comparable to young mice. However, memory was rescued on different days in the Morris water maze; early for hippocampal GluN2B subunit enrichment and later for the frontal lobe. A higher concentration of the GluN2B antagonist, Ro 25-6981, was required to impair long-term spatial memory in aged mice with enhanced GluN2B expression, as compared to aged controls, suggesting there was an increase in the number of GluN2B-containing NMDA receptors. In addition, hippocampal slices from aged mice with increased GluN2B subunit expression exhibited enhanced NMDA receptor-mediated excitatory post-synaptic potentials (EPSP). Treatment with Ro 25-6981 showed that a greater proportion of the NMDA receptor-mediated EPSP was due to the GluN2B subunit in these animals, as compared to aged controls. These

© 2012 Elsevier B.V. All rights reserved.

*Corresponding author: Address of corresponding author Dr. Kathy R. Magnusson, Healthy Aging Program, Linus Pauling Institute, 307 Linus Pauling Science Center, Oregon State University, Corvallis, OR 97331, USA, Tel – 1 (541) 737-6923, Fax – 1 (541) 737-5077, Kathy.Magnusson@oregonstate.edu.

5.1 Disclosure statement

Yes, there is potential conflict of interest. R.H. has a financial interest in Viraquest, Inc., the company that provided the viral vector.

Publisher's Disclaimer: This is a PDF file of an unedited manuscript that has been accepted for publication. As a service to our customers we are providing this early version of the manuscript. The manuscript will undergo copyediting, typesetting, and review of the resulting proof before it is published in its final citable form. Please note that during the production process errors may be discovered which could affect the content, and all legal disclaimers that apply to the journal pertain.

results suggest that increasing the production of the GluN2B subunit in aged animals enhances memory and synaptic transmission. Therapies that enhance GluN2B subunit expression within the aged brain may be useful for ameliorating age-related memory declines.

Keywords

Aging; spatial memory; NMDA receptor; NR2B subunit; C57BL/6 mice; adenoviral vector

1. Introduction

Aging is associated with multiple functional declines, including declines in strength, balance, motor coordination, cognitive flexibility and memory [1, 2]. One of the earliest cognitive functions to show declines with increasing age is memory; deterioration is evident by the fifth decade in humans and is associated with significant impairment in memory recall [3, 4]. Spatial memory, which is responsible for the navigation of organisms within their environment, is particularly affected by the aging process [5–7]. In particular, spatial long-term and delayed short-term memory, as well as cognitive flexibility (i.e. the ability to switch a behavioral response according to the context of a situation), decline with age [8–13].

Specific brain regions are important for the acquisition, consolidation and retrieval of spatial memory, including the hippocampus and the prefrontal cortices within the frontal lobe [14–20]. Specifically, the medial and orbital prefrontal cortices are important for both spatial long-term and short-term memory in the radial arm and Morris water mazes [20, 21]. The frontal lobe has also been shown to be necessary for the encoding of delayed short-term memories, as well as contributing to long-term memory by maintaining the learned information [22, 23]. The medial prefrontal cortex has also been shown to be important for the retrieval of spatial information stored in the hippocampus [24]. The frontal lobe, including the orbital and medial prefrontal cortices, has also been shown to be important for cognitive flexibility [25–28]. In contrast, the hippocampus is responsible for the consolidation of less stable short-term memories into more stable long-term memories, which can be stored in the frontal lobe [19, 29, 30]. In particular, spatial long-term memory has been shown to require the hippocampus in a variety of studies using hippocampal lesions [14, 31–33]. In particular, selective electrolytic lesions of the entorhinal projection to the CA1 disrupt the consolidation of long-term memory [15]. In contrast, lesions of the dentate gyrus (DG) and CA3, suggest that these regions of the hippocampus may be important for the acquisition of spatial memory [16, 17]. The caudate nucleus is also believed to be involved in the acquisition and consolidation of spatial memory in the Morris water maze [34–36]. However, the striatum and medial temporal lobe are also believed to be involved in the formation of associative memory, which does not appear to be affected by aging [37, 38].

One subtype of glutamate receptor, the N-methyl-D-aspartate (NMDA) receptor, is highly expressed throughout the frontal lobe, caudate nucleus and hippocampus [39, 40] and has been shown to be important for learning and memory [41, 42]. Specifically, NMDA receptors are especially important for spatial memory [43] and are also thought to be involved in cognitive flexibility [44]. Antagonists of the receptor block initiation of long-term potentiation (LTP), a cellular mechanism believed to underlie learning and memory, in both the hippocampus and regions of the frontal lobe [45–51]. Memory and learning, including spatial memory, are also impaired by use of NMDA receptor specific antagonists such as AP5, MK801, ketamine and Ro 25-6981 [43, 52–60]. In addition, correlations have

been seen between NMDA-displaceable [^3H] glutamate binding and NMDA subunit expression and spatial memory performance in the Morris water maze [61–67].

Aging animals exhibit declines in NMDA receptor binding densities. A number of binding studies, employing [^3H]glutamate or glutamate analogs, have shown that the NMDA receptors are more susceptible to the effects of aging than any other type of glutamate receptor in the ventrolateral frontal cortex, including orbital and insular cortices, and in the hippocampus of the mouse brain [68–71]. Similar results were also observed in other species, including rats [11, 44, 72], canids [65], non-human primates [66] and humans [73]. Several studies have used spatial memory tasks to characterize the relationship between age-related declines in memory and NMDA receptor expression [8–12, 61, 62, 67, 74–78]. Specifically, the age-related decline in densities of NMDA receptor binding and expression of its subunits in regions of the frontal lobe and hippocampus of the rodent brain have been shown to be associated with declines in spatial memory, including spatial long-term and delayed short-term memory, during aging [8–12, 44, 61, 62, 67, 78].

NMDA receptors are heteromeric tetramers composed of combinations of subunits from different families of proteins, now termed GluN1 (NR1), GluN2 (NR2) and GluN3 (NR3) subunit families [79, 80]. Of the NMDA receptor subunits, the GluN2B subunit is most affected by the aging process. The GluN2B subunit mRNA has been shown to be especially vulnerable to the effects of aging in the cerebral cortex and dentate gyrus of the hippocampus [63, 65]. Significant declines in GluN2B mRNA expression have also been observed in the prefrontal cortex and caudate nucleus of aged macaques and in the hippocampus of aged rats [81, 82]. In the frontal lobes of C57BL/6 mice, it appears that the decline in mRNA during adult aging may be a continuation of the developmental decline and, therefore, may be programmed [64]. Protein expression of the GluN2B subunit also declines with age across regions of the frontal lobe and hippocampus [9, 81, 83]. However, the protein levels of the GluN2B subunit show a greater decline with age within the synaptic membrane of the frontal lobe than in the tissue as a whole [12]. Within the hippocampus, there is a significant decline in GluN2B subunit expression in the synapse with age, similar to the tissue changes [12]. Functional studies of NMDA receptors also suggest that aging results in a decrease in or loss of functional GluN2B-containing receptors. Specifically, NMDA receptors from aged animals appear to be less sensitive to ifenprodil, a GluN2B specific antagonist, and have an increased rate of deactivation (faster channel closing) [84, 85].

The GluN2B subunit has also been shown to be important for spatial memory. Its decrease, via experimental manipulation, has been shown to be sufficient to account for the degree of spatial long-term memory impairment seen in aged rodents [86]. Moreover, aging studies have shown that there is a significant correlation between decreased GluN2B subunit expression and impaired spatial long-term memory in aged animals [9]. Specifically, age-related decreases in the protein expression of the GluN2B subunit within crude synaptosomes of the frontal cortex of C57BL/6 mice show a relationship to the declines in performance in the long-term spatial memory task across age groups. However, those expressing the highest levels of the GluN2B subunit within the synaptic membrane of the hippocampus, among aged mice, are the poorest performers in the same task [12]. Previous research has shown that increasing GluN2B subunit expression throughout multiple brain regions from birth is beneficial to memory, including spatial long-term and delayed short-term memory, and remains beneficial even into middle-age (18 months) [87, 88]. These data suggest that maintaining higher levels of the GluN2B subunit during aging, than are seen in normal aged mice, could be beneficial for memory.

The present paper explored the effects of increasing the expression of the GluN2B subunit within the frontal lobe or the hippocampus of aged mice using a replication deficient adenoviral vector to deliver cDNA specific to the GluN2B subunit. The orbital cortex was targeted because the ventrolateral frontal cortex, which includes the orbital and insular cortices, exhibits consistent declines in GluN2B subunit mRNA during aging in C57BL/6 mice [65] and shows significant relationships between age-related declines in NMDA receptor binding and spatial memory [61]. In addition, the orbital cortex is centrally located within the frontal lobe, which provided the best target for enhancement throughout the lobe.

Adenoviral vectors have previously been used to effectively deliver genes to the central nervous system (CNS) [89]. An adenoviral vector was chosen because of its size (packaging capacity) [90]. Specifically, the GluN2B vector expresses two transgenes, GluN2B and eGFP, from two independent promoters. This cannot be accomplished in an adeno-associated viral vector because the packaging capacity is too small [91]. A lentivector, such as feline immunodeficiency virus (FIV), can be engineered to express two transgenes using an internal ribosomal entry site (IRES) sequence; however, the expression levels of the gene under the control of the IRES is much lower [92]. Finally, higher infectious titers can be obtained with adenoviral vectors, as compared to lentivectors [93].

The purpose of the present study was to determine whether the decline in spatial memory and cognitive flexibility observed during aging could be improved by regionally increasing the expression of the GluN2B subunit within the aged brain. This would help determine whether a therapy aimed at enhancing the number of NMDA receptors that contain the GluN2B subunit during old age would be beneficial to cognitive functions.

2. Methods

2.1 Injection solutions

2.1.1 Adenoviral vectors—Custom adenoviral vectors were designed by Viraquest, Inc. (North Liberty, IA). A plasmid containing the cDNA for the GluN2B subunit, a gift from Dr. M. Mishina, University of Tokyo; was subcloned into a human replication deficient type 5 adenoviral vector with cytomegalovirus (CMV) promoters and reporter gene for enhanced green fluorescent protein (eGFP). The GluN2B vector contains the cDNA of the GluN2B subunit gene and eGFP. The control vector contains only the cDNA of eGFP. The GluN2B vector and control vector were diluted with the A195^{Viraquest} buffer to give a final concentration of approximately 2.0×10^8 PFU/mL. Animals meant for vehicle alone were injected with equivalent volumes of the A195^{Viraquest} buffer.

2.1.2 GluN2B Antagonist—The GluN2B antagonist, Ro 25-6981 (Sigma Aldrich, St. Louis, MO, USA), was diluted in 100% Dimethyl sulfoxide (DMSO) (Sigma Aldrich, St. Louis, MO, USA) to a final concentration of 5 or 10 mg/mL, as previously published [58]. Each mouse received a subcutaneous injection of either 5 or 10 mg/kg Ro 25-6981 or an equivalent volume of DMSO 30 minutes prior to beginning each block of 4 place trials or cued trials. Each mouse received 1–2 injections per day, depending on the task.

2.1.3 Lipopolysaccharide—Adenoviral vectors have been shown to elicit inflammatory responses within the brain [94], so an LPS-induced inflammation model was used as a positive control for assessing inflammation. Lipopolysaccharide from *Escherichia coli* (Sigma Aldrich, St. Louis, Mo) was diluted in sterile water to give a final concentration of 1mg/mL and then stored at -80°C until used.

2.2 Transfection of cells

A laboratory generated cell line of rabbit skin cells were transfected with 2.0×10^9 PFU/mL of either the control vector or the GluN2B vector, followed by an overnight incubation. GFP expression was monitored using a Leica DM LB microscope (Leica Microsystems, Wetzlar, Germany). To visualize GluN2B expression, cells were fixed with methanol and then stained for the GluN2B subunit (refer to section 2.7).

2.3 Animals

A total of two-hundred and thirty-seven male C57BL/6 mice (National Institute on Aging, NIH, Bethesda, MD and The Jackson Laboratories, Bar Harbor, ME) representing 2 different age groups (3 and 22–26 months of age) were used for this study. The animals were fed *ad libitum* and housed individually in micro-isolator cages on a 12/12 hour light/dark cycle. The animals within each age group were randomly divided into two injection groups (frontal or hippocampal) and 3 vector treatment groups, which were injected bilaterally with either: vehicle, control vector, or GluN2B vector. The mice with frontal injections were tested for spatial long-term (2 days) and delayed short-term memory, cognitive flexibility and associative memory (Figure 1). Following hippocampal injections, mice were tested for spatial long-term memory (3 days), cognitive flexibility and associative memory (Figure 1). A separate group of aged mice, which had received bilateral injections of either the GluN2B vector or vehicle solution into the frontal lobe, were randomly divided into 3 antagonist treatment groups. The antagonist treatment groups received subcutaneous injections of 5mg/kg Ro 25-6981, 10mg/kg Ro 25-6981 or DMSO alone 30 minutes prior to every block of 4 place trials for 2 days for spatial long-term memory testing and before the 6 cued trials for associative memory. Following behavioral testing (see below), all of the mice described above were euthanized by exposure to CO₂, followed by decapitation. The brains were removed, frozen on dry ice, and stored at -80°C .

Another separate group of aged mice, which had received bilateral injections of either the GluN2B vector, control vector or vehicle into the hippocampus, were shipped overnight to University of Florida five days post-surgery. Beginning on day 7 after shipping, one mouse per day was euthanized by exposure to isoflurane (Abbott Laboratories, North Chicago, IL) and swiftly decapitated. The hippocampi were removed and used for electrophysiological recording.

2.4 Stereotaxic surgery

All mice underwent stereotaxic surgery and received bilateral injections centered on the orbital cortex, as described by Das et al. with some modifications [95], or the dorsal hippocampus. Anesthesia was induced with 4% isoflurane (Vet One, distributed by MWI, Meridian, ID) and maintained with 1.5–2.25% isoflurane. Holes (1–2 mm) were drilled in the skull using the stereotaxic coordinates 2.58 mm rostral to bregma and ± 1.5 mm lateral to the longitudinal suture for the frontal lobe or 1.70 mm caudal to bregma and ± 1.0 mm lateral to the longitudinal suture for the hippocampus. Injections were delivered 2.3 mm ventral to the skull surface for the left and right ventral orbital cortices and 2.5 mm ventral to the skull surface for the right and left hippocampi. Injections consisted of equivalent volumes (orbital cortices: 5 μ l per injection and hippocampi: 3 μ l per injection) and equivalent concentrations of GluN2B vector, control vector or vehicle. For the mouse receiving lipopolysaccharide, the volume per injection was 1 μ L (1 μ g lipopolysaccharide). The mouse receiving lipopolysaccharide was treated with buprenorphine (0.1mg/kg) every 12 hours until euthanized 4 days post-injection.

2.5 Behavioral testing

2.5.1 Acclimation—Six to seven days post-surgery, mice were acclimated to the water maze for two consecutive days. Each session consisted of each mouse swimming for 60 seconds in the tank without the platform and then being placed on the platform in the tank and trained to remain there for 30 seconds. This platform position was different from those used for memory testing.

2.5.2 Memory and cognitive flexibility testing—Spatial long- and delayed short-term (frontal lobe injections only) memory, cognitive flexibility and associative memory were assessed using the Morris water maze as described previously with some modifications (Figure 1) [95]. Briefly, following acclimation, mice underwent 2 (frontal lobe injections) or 3 (hippocampal injections) days of long-term spatial memory testing and one day of reversal task, in order to assess cognitive flexibility [95]. A delayed short-term spatial memory task was then performed [8], but only for mice who received injections into the frontal lobe. The task consisted of two daily sessions of 4 place trials each. The platform position changed for each session. Trials consisted of a naïve trial ($T_{\text{naïve}}$) followed by a trial after a 10 minute delay, called T_{delay} and 2 more trials at 2 minute delays (not used for evaluation). Trials consisted of 60 seconds maximum in the water searching for the platform and 30 seconds on the platform. Following either the cognitive flexibility task or the delayed short-term spatial memory task, an associative (control) memory task [95] was employed to test motivation, visual acuity, and physical ability for memory testing. For mice that received hippocampal injections, the Atlantis platform (HVS Image Ltd, Twickenham, Middlesex, UK) was used for the escape platform.

2.6 Electrophysiology

2.6.1 Hippocampal slice preparation—The procedure for hippocampal slice preparation and recording has been published previously [96, 97]. Briefly, mice were anesthetized with isoflurane (Abbott Laboratories, North Chicago, IL) and swiftly decapitated. The brains were rapidly removed and the hippocampi were dissected. Hippocampal slices (~ 400 μm) were cut parallel to the alvear fibers using a tissue chopper. The slices were incubated in a holding chamber at room temperature containing artificial cerebrospinal fluid (ACSF) (in mM): NaCl 124, KCl 2, KH_2PO_4 1.25, MgSO_4 2, CaCl_2 2, NaHCO_3 26, and glucose 10. Thirty to sixty min before recording, 2–3 slices were transferred to a standard interface recording chamber (Harvard Apparatus, Boston, MA); the chamber was continuously perfused with standard oxygenated (95% O_2 , 5% CO_2) ACSF at a flow rate of 2 ml/min. The pH and temperature were maintained at 7.4 and $30 \pm 0.5^\circ\text{C}$, respectively. Humidified air (95% O_2 , 5% CO_2) was continuously blown over the slices.

2.6.2 Extracellular recordings—Extracellular field potentials from stratum radiatum of CA1 were recorded with glass micropipettes (4–6 $\text{M}\Omega$) filled with recording medium (ACSF) as published previously [96–105]. Briefly, stimulating electrodes (outer pole: stainless steel, 200 μm diameter; inner pole: Platinum/Iridium, 25 μm diameter, FHC, Bowdoinham, ME) were positioned on either side (approximately 1 mm) of a recording electrode localized to the middle of stratum radiatum and single diphasic stimulus pulses were alternated between pathways such that each pathway was activated at 0.033 Hz. A single diphasic stimulus pulse of 100 μsec was passed via a stimulator (SD9 Stimulator, Grass Instrument Co, West Warwick, RI) to the Schaffer collateral commissural pathway to evoke field potentials at 0.033 Hz. The signals were amplified, filtered between 1 Hz and 1 kHz and stored on computer disk for off-line analysis. To obtain the NMDA receptor-mediated component of the field EPSP, slices were incubated in ACSF containing low extracellular Mg^{2+} (0.5 mM), 6,7-dinitroquinoxaline-2,3-dione (DNQX, 30 μM), and picrotoxin (PTX, 10 μM) [96, 106]. For analyzing the influence of Ro 25-6981 (4 μM) on

NMDA receptor-mediated EPSP, a stable baseline for at least 10 minutes was collected and then Ro-25-6981 was bath applied. The NMDA receptor-mediated synaptic response was obtained for the last 5 min following 60 min bath application of Ro 25-6981.

2.7 Immunohistochemistry

2.7.1 Tissue sectioning—The brain of each animal was cut in half longitudinally and one half (alternating sides across animals) was sectioned coronally using a Leica CM1850 UV Cryostat (Leica Microsystems Inc., Bannockburn, IL). The 20 μm sections were cold-mounted onto plus slides (Thermo Fisher Scientific, Waltham, MA). Brain sections representing at least one animal from each experimental group (age by treatment) were placed on each slide and the order was determined by block design. Slides were kept at -80 degrees Celsius until further processing.

2.7.2 Peptide and antibodies—Representative coronal tissue sections from each animal were labeled with either 20 $\mu\text{g}/\text{mL}$ biotin-conjugated isolectin B₄ (Sigma Aldrich, St. Louis, MO) to visualize microglia (inflammation marker), a 1:100 dilution of an anti-NMDA e2 (GluN2B) goat polyclonal antibody (Santa Cruz Biotechnologies, Santa Cruz, CA), and/or a 1:500 dilution of an anti-glial fibrillary acidic protein (GFAP) antibody (Abcam, Cambridge, MA) to visualize astrocytes or a 1:500 dilution of an anti-neurofilament antibody (Abcam, Cambridge, MA) to visualize neurons or a 1:500 dilution of an anti-GFP antibody (Sigma Aldrich, St. Louis, MO). Secondary antibodies used for visualization included rhodamine-conjugated donkey anti-goat antibody (Millipore, Billerica, MA), fluorescein-conjugated goat anti-rabbit antibody (Millipore, Billerica, MA) or Alexa Fluor 350 goat anti-rabbit antibody (Molecular Probes, Eugene, OR).

2.7.3 Staining protocol—Slides were fixed in 4% paraformaldehyde for 15 min. Slides were treated with 0.3% H₂O₂ solution for 15 min, followed by a 1 hour block in 0.1% BSA (isolectin B₄) or 5% serum (GluN2B or GFAP). Slides were then either incubated in primary antibody or isolectin B₄ for 48 hours. Slides were then treated with either 1:1000 dilution of secondary antibody and/or 1:800 avidin-biotin complex solution (Vectastain Elite ABC kit, Vector Laboratories, Burlingame, CA) for 1 hour each. Slides were visualized with 3,3'-Diaminobenzidine (DAB) (Sigma Fast DAB, Sigma Aldrich, St. Louis, MO) by incubation for either 5 min (isolectin B₄) or 30 min (GluN2B subunit). Nonspecific slides were incubated in either the absence of biotin-conjugated isolectin B₄ or primary antibody. Images were captured using a Leica DM LB microscope and SPOT camera (Diagnostic Instruments Incorporated, Sterling Heights, MI).

2.8 Injection site mapping

Representative coronal (rostral to caudal) sections from each animal were used to map the location of the injection site and the distribution of increased GluN2B expression (or to verify its absence in control animals). All representative sections used for mapping were labeled for GluN2B and visualized with DAB staining.

2.9 Data Analysis

The data for each memory task was analyzed as described earlier with a few modifications [67]. Briefly, the distance of the animal from the platform was measured every 0.2 seconds by the computer for the whole duration of the trial. Cumulative proximity was calculated by summing those distances. Correction for start position was performed using a macro in Excel software (Microsoft Corp., Seattle, WA). A cumulative proximity measurement for the ideal path using the start position, average swim speed and platform position was calculated with the use of this macro. This cumulative proximity measure for the ideal path

was subtracted from the cumulative proximity score for the whole track to obtain the corrected cumulative proximity scores for the place trials in the long-term spatial memory and cognitive flexibility tasks and all trials in delayed short-term and associative memory (control) task. The difference between naïve and delayed trials was calculated from their respective corrected cumulative proximity measurements in the delayed short-term memory tasks. The data for electrophysiology was analyzed as described earlier with a few modifications [96, 97]. Briefly, the input-output curve for the NMDA receptor-mediated EPSP was constructed by measuring the maximum amplitude of the responses for increasing stimulation intensities. Changes in NMDA receptor-mediated EPSP induced by application of Ro 25-6981 were calculated as the percent change from the averaged baseline responses collected 10 min before drug application. Animals were removed from the study if they consistently floated throughout trials (1 mouse), performed significantly worse in cued trials from the rest of the animals (greater than the mean plus two standard deviations; 5 mice) or if there was considerable difference in injection location and protein expression from their counterparts (15 mice). These excluded animals were from both ages and most treatment groups.

2.10 Statistical Analysis

The data for memory tasks were statistically analyzed by Analysis of Variance (ANOVA) or one sample T- test using Statview software 5.0 (SAS Institute). Performance in long-term spatial memory, cognitive flexibility, delayed short-term spatial memory and associative memory tasks were analyzed separately by repeated measures ANOVA and two-way ANOVA followed by Fisher's protected least significant difference post-hoc analysis as indicated. Analysis of place trials within days was planned because of previous work showing greater age differences on day 2 [9]. The response variable was performance in behavioral trials while the independent variables were age and/or treatment. NMDA receptor-mediated EPSP responses in hippocampal slices were analyzed separately by repeated measures ANOVA and two-way ANOVA followed by Fisher's protected least significant difference post-hoc analysis or one sample T-test as indicated. The response variable was NMDA receptor-mediated EPSP response or percent change from NMDA receptor-mediated EPSP response compared to baseline while the independent variable was treatment. For all comparisons, only $p < 0.05$ were considered statistically significant.

3. Results

3.1 Effect of the GluN2B vector in the frontal lobe on spatial and associative memory

There was an overall effect of age on cumulative proximity scores in place trials within the long-term spatial memory task, with young animals spending more time closer to the platform than aged animals ($F_{(1,76)}=26.3$, $p<0.0001$; young= 6546 ± 1092 cm, aged= 9435 ± 1172 cm). There was also an age by treatment interaction ($F_{(2,76)}=4.7$, $p=0.01$). For the cognitive flexibility task, where the location of the platform was moved to the opposite quadrant from that used in the long-term spatial memory task, there was an overall significant effect of age on cumulative proximity scores ($F_{(1,76)}=3.8$, $p=0.05$; young= 4443 ± 957 cm, aged= 5581 ± 988 cm), with young animals spending more time closer to the platform. The average difference in cumulative proximity between $T_{\text{naïve}}$ and T_{delay} trials over 16 sessions was used to evaluate spatial short-term memory with a 10 minute delay. There was an overall significant effect of age on cumulative proximity ($F_{(1,76)}=11.3$, $p=0.0012$; young= 2231 ± 299 cm, aged= 1103 ± 506 cm), with young animals having greater differences between the naïve and delayed trials than old. Within the associative memory (control) task, all spatial cues were removed and the platform position was made visible with a flag as a cue to its position for the cued trials. For this control task, there was no overall

significant effect of treatment across ages ($F_{(1,76)}=0.6$, $p=0.44$; young= 870 ± 243 cm, aged= 874 ± 275 cm).

There was a significant interaction between age and treatment in place trials and probes ($F_{(2,75)}=3.5$, $p=0.03$). Therefore, the young and aged mice were analyzed separately for treatment effects. Comparisons between aged treatments and young vehicle treatment were included to assess the degree of improvement. There were no significant effects of treatment on the young mice in any of the behavioral tasks (Supplemental Table 1 $p=0.15$ – 0.87), with the exception of the probe trial at the end of the first day of spatial long-term memory. Young mice treated with the GluN2B vector showed a higher average proximity to the platform location compared to either young control group by the end of the first day ($p=0.02$ – 0.025 ; vehicle= 37 ± 3 cm, control vector= 38 ± 2 cm, GluN2B vector= 55 ± 9 cm). However, their average proximity scores for the platform location were similar to the young control animals by the end of the second day ($p=0.60$ – 0.79 , vehicle= 33 ± 3 cm, control vector= 31 ± 2 cm, GluN2B vector= 36 ± 10 cm).

For aged mice, there was an overall significant effect of treatment across blocks of four place trials (Fig. 2A, $F_{(2,37)}=3.3$, $p=0.05$) and a significant interaction between treatments and blocks of place trials (Fig. 2A, $F_{(6,111)}=3.8$, $p=0.0016$). Aged mice treated with the GluN2B vector had significantly lower cumulative proximity scores than both of the aged control groups by the second day of long-term spatial memory trials (Fig. 2B, $p=0.001$ – 0.015). The cumulative proximity scores of the aged GluN2B vector-treated mice were similar to the cumulative proximity scores of the young vehicle-treated mice by the second day (Fig. 2B, $F_{(1,27)}=0.6$, $p=0.44$). Young vehicle-treated mice had significantly lower proximity scores than aged control vector-treated mice in day 1 of long-term spatial memory trials and significantly lower proximity scores than both aged control groups by the second day (Fig. 2B, p 0.0001– 0.0016).

Within probe trials, aged mice treated with the GluN2B vector exhibited lower average proximity to the platform location compared to either aged control group by the end of the second day (Fig. 2C, Pr2; $p=0.0006$ – 0.05). The average proximity to the platform location of aged mice treated with the GluN2B vector was similar to young vehicle-treated animals by the end of the second day (Fig. 2C, $F_{(1,27)}=0.45$, $p=0.51$). There was no significant effect of treatment in aged mice on average swim speed ($F_{(2,37)}=2.3$, $p=0.11$; aged vehicle: 14.4 ± 0.3 cm/sec, aged control vector: 15.1 ± 0.5 cm/sec, aged GluN2B vector: 15.8 ± 0.5 cm/sec).

There were no significant effects of treatment on cumulative proximity in reversal trials in the aged animals (Fig. 2D, $F_{(2,37)}=0.01$, $p=0.99$). There was no overall significant effect of treatment on the average difference in cumulative proximity between trials with a 10 minute delay in aged animals (Fig. 2E, $F_{(2,37)}=0.3$, $p=0.73$). Within the associative memory (control) task, there was no significant effect of treatment within aged animals (Fig. 2F, $F_{(2,37)}=2.3$, $p=0.12$). There was also no overall significant difference in the cumulative proximity scores in the control task between young vehicle-treated animals and aged GluN2B vector-treated animals (Fig. 2F, $F_{(1,27)}=1.0$, $p=0.33$) or aged controls ($p=0.13$ – 0.54).

3.2 Effect of a GluN2B antagonist on long-term spatial and associative memory

Aged mice, treated with either GluN2B vector or vehicle within their frontal lobe, were treated systemically with the GluN2B specific antagonist, Ro 25-6981. This was designed to determine whether the increased expression of the GluN2B subunit was responsible for the improved long-term spatial memory observed in aged mice. Systemic delivery of this GluN2B specific antagonist has previously been shown to impair object recognition memory

[58]. Due to the previous results with enhanced GluN2B expression in the frontal lobe, the focus for the antagonist study was on the second day of spatial long-term memory testing. There were overall significant effects of antagonist treatment (Fig. 3A–B, $F_{(2,47)}=4.5$, $p=0.02$), and a significant vector by antagonist interaction (Fig. 3A–B, $F_{(2,47)}=3.1$, $p=0.05$). Aged vehicle-treated animals that received 5mg/kg Ro 25-6981 had significantly higher cumulative proximity scores than vehicle-treated dimethyl sulfoxide (DMSO) animals (Fig. 3B, $p=0.002$) in the second day. However, aged GluN2B vector-treated animals that received 5mg/kg Ro 25-6981 had similar cumulative proximity scores to GluN2B vector-treated DMSO animals (Fig. 3B, $p=0.22$). There was a near significant difference in cumulative proximity between aged vehicle-treated animals that received 5mg/kg Ro 25-6981 compared to GluN2B vector-treated animals that received the same dose of Ro 25-6981, with GluN2B vector treated- animals spending more time closer to the platform than vehicle-treated animals (Fig. 3B, $F_{(1,15)}=3.5$ $p=0.08$). Aged GluN2B vector-treated mice that received a higher dose of Ro 25-6981 (10 mg/kg) spent less time near the platform than either aged GluN2B vector-treated DMSO (Fig. 3B, $p=0.002$) or aged GluN2B vector-treated animals that received a lower dose of Ro 25-6981 (5 mg/kg) (Fig. 3B, $p=0.03$). Aged GluN2B vector-treated animals that received the higher dose of Ro 25-6981 (10 mg/kg) had similar cumulative proximity scores to aged vehicle-treated mice that received the lower dose of Ro 25-6981 (5 mg/kg) (Fig. 3B, $F_{(1,12)}=0.63$, $p=0.44$). Within the associative memory (control) task, there were no significant effects of either vector treatment (Fig. 3C, $F_{(1,45)}=0.05$, $p=0.83$) or antagonist treatment (Fig. 3C, $F_{(2,45)}=0.08$, $p=0.93$) and no significant vector by antagonist interaction (Fig. 3C, $F_{(2,45)}=0.01$, $p=0.99$).

3.3 Effect of the GluN2B vector in the hippocampus on spatial and associative memory

There was an overall effect of age on cumulative proximity in the long-term spatial memory task, with young animals spending more time closer to the platform than aged animals ($F_{(1,59)}=28.9$, $p<0.0001$; young= 4702 ± 737 cm, aged= 6863 ± 835 cm). For the cognitive flexibility task, there was an overall significant effect of age on cumulative proximity ($F_{(1,59)}=27.2$, $p<0.0001$; young= 3982 ± 1036 cm, aged= 6448 ± 1043 cm), with young animals having lower proximity scores than aged animals. Within the associative memory (control) task, all spatial cues were removed and the platform position was cued with a flag. There was no overall significant effect of age ($F_{(1,58)}=0.77$, $p=0.38$; young= 3057 ± 880 cm; aged= 2663 ± 752 cm) or treatment ($F_{(2,58)}=0.33$, $p=0.72$) across associative memory trials.

There were significant interactions between age or treatment and blocks of place trials in the spatial long-term memory trials ($p=0.0003$ – 0.004). In order to make comparison between treatments, each age group was analyzed separately. Comparisons between aged treatments and young vehicle treatment were included to assess the degree of improvement. There were no significant effects of treatment on the young mice in any of the behavioral tasks (Supplemental Table 1 $p=0.11$ – 0.97).

Within aged mice, there was no overall effect of treatment across blocks of four place trials (Fig. 4A–B, $F_{(2,33)}=0.66$, $p=0.52$) but there was a significant interaction of treatment by blocks of four place trials (Fig. 4A–B, $F_{(10,165)}=3.1$, $p=0.0012$). Aged mice treated with the GluN2B vector had lower cumulative proximity scores than both of the aged control groups in the first day of long-term spatial memory trials (Fig. 4B, $p=0.002$ – 0.05). The cumulative proximity scores of aged mice treated with the GluN2B vector for the first day were not significantly different from those of young vehicle-treated mice (Fig. 4B, $F_{(1,26)}=1.2$, $p=0.29$). However, for aged mice treated with the GluN2B vector there was a trend for higher cumulative proximity scores in later trials compared to aged controls (Fig. 4A). For days 2 and 3, aged GluN2B vector-treated mice had higher cumulative proximity scores, as compared to young vehicle-treated animals (Fig. 4A–B, $p=0.004$ – 0.03). For probe trials, there was no overall effect of treatment on average proximity scores for aged animals (Fig.

4C, $p=0.06-0.77$). In the flexibility task, there was no significant effect of treatment on cumulative proximity scores within aged animals (Fig. 4D, $F_{(2,33)}=0.68$, $p=0.52$). There was no significant effect of treatment on cumulative proximity scores within aged (Fig. 4E, $F_{(2,33)}=0.29$, $p=0.75$) in the associative memory (control) task.

3.4 Effect of the GluN2B vector in the hippocampus on NMDA receptor-mediated EPSP

There was an overall effect of treatment on NMDA receptor-mediated EPSPs in hippocampal slices, with slices from aged GluN2B vector-treated animals exhibiting higher NMDA receptor-mediated EPSP than those from aged controls (Fig. 5A, $F_{(2,28)}=7.6$, $p=0.0024$). There was also a significant interaction of treatment by stimulation strength (Fig. 5A, $F_{(22,308)}=5.7$, $p<0.0001$). Hippocampal slices from aged mice treated with the GluN2B vector had greater NMDA receptor-mediated EPSP than either of the aged controls at higher stimulation strengths (14–32 volts; Fig. 5A, $p=0.002-0.02$) but not at lower stimulation strengths (4–12 volts; Fig. 5A, $p=0.07-0.2$). One sample t-tests were used to examine changes in the NMDA receptor-mediated synaptic response for the last 5 min following 60 min bath application of Ro 25-6981. The results reveal that only mice treated with the GluN2B vector exhibited a significant ($p = 0.03$) decrease compared to baseline (Fig. 5B).

3.5 Effect of vectors on GluN2B protein expression

The efficacy of the adenoviral vectors used was first confirmed *in vitro*. Rabbit skin cells were transfected with the GluN2B vector and expressed both the GluN2B subunit and GFP, which co-localized (Supplemental Fig. 1A–C). Rabbit skin cells transfected with the control vector only expressed GFP only (Supplemental Fig. 1D–E). *In vivo*, there was increased GluN2B immunoreactivity within the frontal lobe, corpus callosum, and caudate nucleus for the frontal lobe injections and within the hippocampus and corpus callosum for the hippocampal injections in mice treated with the GluN2B vector as compared to endogenous expression (Fig. 6C, F; Fig. 7C, F, I, J, K). Preliminary studies showed peak expression *in vivo* around day 10 post-surgery (data not shown). Neither control treatments, vehicle (Fig. 6A, D; Fig. 7A, D, G) or control vector (Fig. 6B, E; Fig. 7B, E, H) elicited a change in GluN2B immunoreactivity from endogenous expression. Increased GluN2B expression was visible in, but was not restricted to, neurons and neuronal processes (Fig. 6C, F; Fig. 7C, F, I, J, K; Fig. 8). GFAP-positive cells also showed enhanced GluN2B immunoreactivity (Fig. 6F; Fig. 7I, J, K). There was lipofuscin (yellow profiles) present in the images of aged brains (Fig. 6A–F, Fig. 7A–I). Injection site mapping of strongly labeled cells following the frontal lobe injections indicated that increased GluN2B expression was predominantly localized to the frontal lobe, including the orbital and motor cortices, but was also seen in the corpus callosum, the caudate nucleus and in the ependymal cells lining the lateral ventricles (Fig. 9). Injection site mapping of strongly labeled cells following the hippocampal injections indicated that increased GluN2B expression was restricted to the corpus callosum, subregions of the hippocampus, including the dentate gyrus and CA1 region, and in the ependymal cells lining the dorsal 3rd ventricle and lateral ventricles (Fig. 10).

3.6 No effect of vectors on inflammation

Since adenoviral vectors have been shown to elicit an inflammatory response within brain tissue [94], representative coronal sections from each age and treatment were stained with an isolectin specific for microglia [107]. Microglia are a marker of inflammation, and is evident in tissue from the frontal lobe of a young mouse (positive control) that received bilateral injections of lipopolysaccharide from *Escherichia coli* into the frontal lobe (Fig. 11D). There was no appreciable difference in inflammation within the injection sites across brain regions or treatments (Fig. 11A–C, E–G). Tissue from vector-treated animals exhibited inflammation comparable to vehicle-treated animals (Fig. 11A–C, E–G). There was no visible difference between aged or young vehicle-treated animals (data not shown).

4. Discussion

This study provides compelling evidence that increasing the expression of the GluN2B subunit of the NMDA receptor within the frontal lobe, caudate nucleus and hippocampus of aged mice can improve synaptic transmission and memory. Aged mice with enhanced GluN2B expression across these brain regions exhibited superior long-term spatial memory over their aged counterparts, and exhibited memory similar to young mice, but on different days of training for the different injection regions. In the hippocampus, enhancing the expression of the GluN2B subunit increased NMDA receptor-mediated synaptic transmission. This suggests that increasing expression of the GluN2B subunit can improve synaptic function and plasticity in the aged brain.

Aged mice with enhanced GluN2B expression across the frontal lobe and rostradorsal caudate nucleus improved learning in the second day of long-term memory training, as compared to aged controls, and the improved performance was similar to that seen in young vehicle-treated mice. By the end of the second day of the long-term spatial memory task, these aged mice showed a stronger bias for the platform location compared to either aged control and, in fact, showed a similar bias for the platform location as compared to young vehicle-treated mice. In contrast, aged mice with increased GluN2B expression in the hippocampus exhibited improved early learning in the first day of the long-term spatial memory task compared to aged controls, and performed similarly to young vehicle-treated mice only on the first day. However, enhanced expression of the GluN2B subunit within the hippocampus of the aged brain did not improve spatial bias development. This could be due to the fact that memory was enhanced early in learning trials but plateaued by the end of the second day. Immunohistochemistry revealed increased GluN2B expression within cells with either neuronal or glial characteristics across the frontal lobe, caudate nucleus and hippocampus of aged mice treated with the GluN2B vector compared to control treatments. Multiple neuronal processes showed enhanced GluN2B expression, suggesting that it was enriched within dendrites, which is where excitatory synapses predominate. Aged mice with enhanced GluN2B subunit expression in the hippocampus exhibited enhanced NMDA receptor-mediated EPSP responses and a larger proportion of that EPSP was blocked by antagonism of GluN2B subunits than was seen with the controls. Together, these data suggest that the adenoviral vector effectively induced increased production of the GluN2B subunit and that aged animals with enhanced expression of the GluN2B subunit exhibited enhanced NMDA receptor-mediated EPSP responses as well as improved learning and retention in a long-term spatial memory task, comparable to young mice.

To confirm and expand these findings, a highly selective and activity-dependent GluN2B antagonist specific for GluN2B-containing receptors, Ro 25-6981 [108] was administered directly to hippocampal slices or systemically to aged mice with enhanced GluN2B subunit expression. This was done in order to determine whether the increased expression of the GluN2B subunit was responsible for the enhanced NMDA receptor mediated EPSP responses observed or improved memory observed in aged mice with enhanced GluN2B subunit expression. Ro 25-6981 has previously been shown to reduce NMDA receptor-mediated EPSP responses and LTP in hippocampal slices or hippocampal slice cultures [109–112]. Direct injection and/or systemic delivery of Ro 25-6981 has previously been shown to impair memory performance in the Morris water maze and object recognition tasks [52, 58–60]. However, it should be noted that other studies suggest that systemic delivery of Ro256981 may not impair spatial learning in the Morris water maze or object recognition memory [113, 114].

Aged mice with enhanced GluN2B subunit expression in the hippocampus exhibited enhanced NMDA receptor-mediated EPSPs. Treatment with the GluN2B antagonist, Ro

25-6981, showed that a greater proportion of the NMDA receptor-mediated EPSP was due to GluN2B subunit component in aged animals with enhanced GluN2B expression compared aged controls. A dose of 5mg/kg of Ro 25-6981 was sufficient to impair spatial long-term memory in aged vehicle-treated mice compared to control on the second day of trials. However, an increased dose (10mg/kg) was required to impair spatial long-term memory in aged mice with enhanced GluN2B expression in the frontal lobe compared to control, and to impair memory similarly to aged vehicle-treated mice that received only a 5mg/kg dose of Ro 25-6981. The lack of difference between the GluN2B vector- and vehicle-injected mice treated with DMSO appeared to be due to trends for a change in performance of both groups from the first experiment. This may be due to the administration of subcutaneous injections of DMSO, which can increase nociception [115]. Also, increased expression of the GluN2B subunit has been associated with increased sensitization to pain in GluN2B-enhanced animals [116], which may explain the worsening of performance in the GluN2B vector-injected mice. There was, however, an overall trend for better performance in the GluN2B vector-treated animals injected with the 5 mg/kg dose of Ro 25-6981 than the vehicle-treated animals receiving the same antagonist dose. In addition, a higher concentration of the GluN2B antagonist, Ro 25-6981, was required to impair long-term spatial memory in aged mice with enhanced GluN2B expression, as compared to aged controls. Antagonism with Ro 25-6981 in hippocampal slices suggests that the observed enhancement in NMDA receptor-mediated EPSP response in aged animals was due to enhanced GluN2B subunit expression. The need for a higher dose of Ro 25-6981 to impair memory in aged mice with enhanced GluN2B expression in the frontal lobe provides further evidence that it was the increased expression of the GluN2B subunit within the brains of aged mice that was responsible for superior memory. These data also suggest that there was an enhancement of GluN2B-containing NMDA receptors within the aged brain.

Memory tasks in the Morris water maze involve acquisition, consolidation and/or retrieval of spatial memories [117]. The acquisition of long-term memories has been shown to occur early in training sessions in the Morris water maze and can be blocked by the application of protein synthesis inhibitors prior to training sessions [118]. In contrast, consolidation of long-term memories has been shown to occur within several hours to days after a training session for a memory task and can be extinguished by the application of protein synthesis inhibitors following training sessions [119]. The NMDA receptor has been shown to be involved in both the acquisition and consolidation of spatial memories in the Morris water maze by blockade with the NMDA receptor antagonist 2-amino-5-phosphonopentanoic acid [120]. Specifically, NMDA receptors within the CA1 region of the hippocampus have been shown to be necessary to the acquisition of spatial memories. This may suggest that the improvement in learning seen within the first day of long-term spatial memory trials (2 hour period) in aged mice with enhanced GluN2B subunit expression in the hippocampus was the result of improved acquisition. By contrast, lesions studies within the orbital cortex have been shown to impair consolidation of spatial memory within the Morris water maze suggesting a role for the frontal lobe in memory consolidation [121]. Moreover, transgenic mice designed to express high levels of the GluN2B subunit throughout the brain, including all regions of the frontal lobe and caudate nucleus, exhibit improved learning on the second day of learning trials [87]. These data may suggest that the enhanced learning observed in the second day of long-term spatial memory trials in aged with increased GluN2B expression in the frontal lobe and caudate nucleus was the result of improved consolidation. Our results suggest that enhancing GluN2B subunit expression within the hippocampus of aged mice might improve early learning, possibly memory acquisition, while expression in the frontal lobe and caudate nucleus might help with later learning, possibly memory consolidation and/or later acquisition. A more global enhancement of this subunit throughout the brain may improve both phases of learning and will be the focus of future studies.

The GluN2B subunit of the NMDA receptor is important to channel kinetics and in regulation of glutamate transmission at developing synapses [122, 123]. Pharmacological and genetic blockade of the GluN2B subunit within the prefrontal cortex results in diminished LTP and impaired fear conditioning [124]. Region specific knockouts of the GluN2B subunit show that expression of the GluN2B subunit within the neocortex and CA1 region of the hippocampus contributes to NMDA receptor-mediated EPSP responses and is necessary for LTP and long-term depression (LTD), and learning and memory in spatial and fear conditioning tasks [125]. Moreover, transgenic mice designed to express higher levels of the GluN2B subunit from birth also exhibit enhanced NMDA receptor-mediated EPSP responses and LTP as well as possess superior memory across adulthood to middle-age [87, 88]. Based on the above findings, the enhanced expression of GluN2B subunit within the aged brain could account for the enhanced NMDA receptor-mediated EPSP responses and superior memory observed in aged mice in this study.

There was no significant effect of treatment on the performance of young mice in any memory task; and enhanced expression of the GluN2B subunit did not improve cognitive flexibility or delayed short-term spatial memory in aged mice. However, transgenic mice designed to express high levels of the GluN2B subunit during development through adulthood possess superior memory compared to wild type [87]. In addition, both the frontal lobe and hippocampus have been shown to be important for cognitive flexibility in rodents [25, 126] and both the NMDA receptor and the GluN2B subunit have been shown to be necessary for cognitive flexibility [44, 127]. Regions of the frontal lobe, such as the dorsomedial prefrontal cortex, have also been shown to be important to delayed short-term spatial memory [128]. Increased expression of the GluN2B subunit across brain regions has been implicated in improved short-term spatial memory [109, 129]. In light of these data, the present results could suggest that the increase in GluN2B expression, or its localization, was not sufficient to improve memory in young mice or improve short-term spatial memory and cognitive flexibility in aged animals.

4.1 Conclusions

In conclusion, increasing the expression of the GluN2B subunit of the NMDA receptor in the frontal lobe or hippocampus appeared to restore long-term spatial memory of aged mice back to the level of young, rescuing it in different phases of learning in a region specific manner. Moreover, aged mice with enhanced GluN2B subunit expression in the hippocampus exhibited enhanced NMDA receptor-mediated EPSP responses. This study further substantiates the important role of the GluN2B subunit in long-term memory and its potential region-specific role in learning and memory. The present work also shows the importance of the decline of the GluN2B subunit to the memory loss that occurs with aging. Moreover, the evidence provided by this study suggests that a therapeutic aimed at enhancing the number or function of the GluN2B containing NMDA receptors in old age could potentially be used to effectively ameliorate memory loss.

Supplementary Material

Refer to Web version on PubMed Central for supplementary material.

Acknowledgments

We thank M. Mishina, University of Tokyo, for the gift of the plasmid containing the cDNA of the GluN2B subunit and V. Elias, M. Shumaker, R. Bochart, C. Lehmann, O. La Faix and R. Jensen for their technical assistance. This work was funded by NIH grant AG016322 to K.R.M. and by NIH Grants AG014979, AG037984, AG036800 and the Evelyn F. McKnight Brain Research Grant to T.C.F.

References

1. Timiras, PS. The nervous system: Functional changes. In: Timiras, PS., editor. *Physiological Basis of Aging and Geriatrics*. Boca Raton: CRC Press; 2003. p. 119-40.
2. Albert, MS. Age-related changes in cognitive function. In: Albert, ML.; JEK, editors. *Clinical Neurology of Aging*. New York City: Oxford University Press; 1994. p. 314-28.
3. Albert, MS.; Funkenstein, HH. The effects of age: Normal variation and its relation to disease. In: Asbury, AK.; McKhann, GM.; McDonald, WI., editors. *Diseases of the Nervous System: Clinical Neurobiology*. Philadelphia: Saunders; 1992. p. 598-611.
4. Singh-Manoux A, Kivimaki M, Glymour M, Elbaz A, Berr C, Ebmeier KP, et al. Timing of onset of cognitive decline: results from Whitehall II prospective cohort study. *BMJ*. 2012; 344:1–8.
5. Perlmuter M, Metzger R, Nezworski T, Miller K. Spatial and temporal memory in 20 to 60 year olds. *J Gerontol*. 1981; 36:59–65. [PubMed: 7451838]
6. Barnes CA, Nadel L, Honig WK. Spatial memory deficit in senescent rats. *Can J Psychol*. 1980; 34:29–39. [PubMed: 7388694]
7. Barnes CA. Aging and the physiology of spatial memory. *Neurobiol Aging*. 1988; 9:563–8. [PubMed: 3062467]
8. Magnusson KR, Scruggs B, Aniya J, Wright KC, Ontl T, Xing Y, et al. Age-related deficits in mice performing working memory tasks in a water maze. *Behav Neurosci*. 2003; 117:485–95. [PubMed: 12802877]
9. Magnusson KR, Scruggs B, Zhao X, Hammersmark R. Age-related declines in a two-day reference memory task are associated with changes in NMDA receptor subunits in mice. *BMC Neurosci*. 2007; 8:43. [PubMed: 17587455]
10. Pellemounter MA, Beatty G, Gallagher M. Hippocampal 3H-CPP binding and spatial learning deficits in aged rats. *Psychobiology*. 1990; 18:298–304.
11. Nicolle MM, Bizon JL, Gallagher M. *In vitro* autoradiography of ionotropic glutamate receptors in hippocampus and striatum of aged Long-Evans rats: Relationship to spatial learning. *Neuroscience*. 1996; 74:741–56. [PubMed: 8884770]
12. Zhao X, Rosenke R, Kronemann D, Brim B, Das SR, Dunah AW, et al. The effects of aging on N-methyl-D-aspartate receptor subunits in the synaptic membrane and relationships to long-term spatial memory. *Neuroscience*. 2009; 162:933–45. [PubMed: 19446010]
13. Schoenbaum G, Setlow B, Saddoris MP, Gallagher M. Encoding changes in orbitofrontal cortex in reversal-impaired aged rats. *J Neurophysiol*. 2006; 95:1509–17. [PubMed: 16338994]
14. Morris RGM, Garrud P, Rawlins JNP, O'Keefe J. Place-navigation impaired in rats with hippocampal lesions. *Nature*. 1982; 297:681–3. [PubMed: 7088155]
15. Remondes M, Schuman EM. Role for a cortical input to hippocampal area CA1 in the consolidation of a long-term memory. *Nature*. 2004; 431:699–703. [PubMed: 15470431]
16. Steffenach HA, Sloviter RS, Moser EI, Moser MB. Impaired retention of spatial memory after transection of longitudinally oriented axons of hippocampal CA3 pyramidal cells. *Proc Natl Acad Sci U S A*. 2002; 99:3194–8. [PubMed: 11867718]
17. Jerman T, Kesner RP, Hunsaker MR. Disconnection analysis of CA3 and DG in mediating encoding but not retrieval in a spatial maze learning task. *Learn Mem*. 2006; 13:458–64. [PubMed: 16882862]
18. Spiers HJ, Maguire EA. The neuroscience of remote spatial memory: a tale of two cities. *Neuroscience*. 2007; 149:7–27. [PubMed: 17850977]
19. Maviel T, Durkin TP, Menzaghi F, Bontempi B. Sites of neocortical reorganization critical for remote spatial memory. *Science*. 2004; 305:96–9. [PubMed: 15232109]
20. Kolb B, Buhrmann K, McDonald R, Sutherland RJ. Dissociation of the medial prefrontal, posterior parietal, and posterior temporal cortex for spatial navigation and recognition memory in the rat. *Cereb Cortex*. 1994; 4:664–80. [PubMed: 7703691]
21. Kolb B, Sutherland RJ, Whishaw IQ. A comparison of the contributions of the frontal and parietal association cortex to spatial localization in rats. *Behav Neurosci*. 1983; 97:13–27. [PubMed: 6838719]

22. Kessels RP, Postma A, Wijnalda EM, de Haan EH. Frontal-lobe involvement in spatial memory: evidence from PET, fMRI, and lesion studies. *Neuropsychol Rev.* 2000; 10:101–13. [PubMed: 10937918]
23. Granon S, Vidal C, Thinus-Blanc C, Changeux JP, Poucet B. Working memory, response selection, and effortful processing in rats with medial prefrontal lesions. *Behav Neurosci.* 1994; 108:883–91. [PubMed: 7826511]
24. Jo YS, Park EH, Kim IH, Park SK, Kim H, Kim HT, et al. The medial prefrontal cortex is involved in spatial memory retrieval under partial-cue conditions. *J Neurosci.* 2007; 27:13567–78. [PubMed: 18057214]
25. de Bruin JP, S-SF, Heinsbroek RP, Donker A, Postmes P. A behavioural analysis of rats with damage to the medial prefrontal cortex using the Morris water maze: evidence for behavioural flexibility, but not for impaired spatial navigation. *Brain Res.* 1994; 652:323–33. [PubMed: 7953746]
26. Bissonette GB, Martins GJ, Franz TM, Harper ES, Schoenbaum G, Powell EM. Double dissociation of the effects of medial and orbital prefrontal cortical lesions on attentional and affective shifts in mice. *J Neurosci.* 2008; 28:11124–30. [PubMed: 18971455]
27. Kim J, Ragozzino ME. The involvement of the orbitofrontal cortex in learning under changing task contingencies. *Neurobiol Learn Mem.* 2005; 83:125–33. [PubMed: 15721796]
28. Barense MD, Fox MT, Baxter MG. Aged rats are impaired on an attentional set-shifting task sensitive to medial frontal cortex damage in young rats. *Learn Mem.* 2002; 9:191–201. [PubMed: 12177232]
29. Takehara K, Kawahara S, Kirino Y. Time-dependent reorganization of the brain components underlying memory retention in trace eyeblink conditioning. *J Neurosci.* 2003; 23:9897–905. [PubMed: 14586019]
30. Frankland PW, Bontempi B, Talton LE, Kaczmarek L, Silva AJ. The involvement of the anterior cingulate cortex in remote contextual fear memory. *Science.* 2004; 304:881–3. [PubMed: 15131309]
31. McNaughton BL, Barnes CA, Meltzer J, Sutherland RJ. Hippocampal granule cells are necessary for normal spatial learning but not for spatially-selective pyramidal cell discharge. *Experimental Brain Research.* 1989; 76:485–96.
32. Olton DS, Walker JA, Gage FH. Hippocampal connections and spatial discrimination. *Brain Research.* 1978; 139:295–308. [PubMed: 624061]
33. Aggleton JP, Hunt PR, Rawlins JN. The effects of hippocampal lesions upon spatial and non-spatial tests of working memory. *Behavioural Brain Research.* 1986; 19:133–46. [PubMed: 3964405]
34. Whishaw IQ, Funk DR, Hawryluk SJ, Karbasheski ED. Absence of sparing of spatial navigation, skilled forelimb and tongue use and limb posture in the rat after neonatal dopamine depletion. *Physiol Behav.* 1987; 40:247–53. [PubMed: 3114777]
35. Setlow B, McGaugh JL. Involvement of the posteroventral caudate-putamen in memory consolidation in the Morris water maze. *Neurobiol Learn Mem.* 1999; 71:240–7. [PubMed: 10082643]
36. Devan BD, Goad EH, Petri HL. Dissociation of hippocampal and striatal contributions to spatial navigation in the water maze. *Neurobiol Learn Mem.* 1996; 66:305–23. [PubMed: 8946424]
37. Mattfeld AT, Stark CE. Striatal and medial temporal lobe functional interactions during visuomotor associative learning. *Cereb Cortex.* 2011; 21:647–58. [PubMed: 20688877]
38. Rapp PR, Rosenberg RA, Gallagher M. An evaluation of spatial information processing in aged rats. *Behav Neurosci.* 1987; 101:3–12. [PubMed: 3828055]
39. Watanabe M, Inoue Y, Sakimura K, Mishina M. Distinct distributions of five N-methyl-D-aspartate receptor channel subunit mRNAs in the forebrain. *J Comp Neurol.* 1993; 338:377–90. [PubMed: 8113446]
40. Rigby M, Le Bourdelles B, Heavens RP, Kelly S, Smith D, Butler A, et al. The messenger RNAs for the N-methyl-D-aspartate receptor subunits show region-specific expression of different subunit composition in the human brain. *Neuroscience.* 1996; 73:429–47. [PubMed: 8783260]

41. Collingridge G. Synaptic plasticity. The role of NMDA receptors in learning and memory. *Nature*. 1987; 330:604–5. [PubMed: 2825035]
42. Butelman ER. A novel NMDA antagonist, MK-801, impairs performance in a hippocampal-dependent spatial learning task. *Pharmacol Biochem Behav*. 1989; 34:13–6. [PubMed: 2696982]
43. Morris RG. Synaptic plasticity and learning: selective impairment of learning rats and blockade of long-term potentiation in vivo by the N-methyl-D-aspartate receptor antagonist AP5. *J Neurosci*. 1989; 9:3040–57. [PubMed: 2552039]
44. Nicolle MM, Baxter MG. Glutamate receptor binding in the frontal cortex and dorsal striatum of aged rats with impaired attentional set-shifting. *Eur J Neurosci*. 2003; 18:3335–42. [PubMed: 14686906]
45. Escobar ML, Alcocer I, Bermudez-Rattoni F. In vivo effects of intracortical administration of NMDA and metabotropic glutamate receptors antagonists on neocortical long-term potentiation and conditioned taste aversion. *Behav Brain Res*. 2002; 129:101–6. [PubMed: 11809500]
46. Castro-Alamancos MA, Donoghue JP, Connors BW. Different forms of synaptic plasticity in somatosensory and motor areas of the neocortex. *J Neurosci*. 1995; 15:5324–33. [PubMed: 7623155]
47. Trepel C, Racine RJ. Long-term potentiation in the neocortex of the adult, freely moving rat. *Cereb Cortex*. 1998; 8:719–29. [PubMed: 9863699]
48. Harris EW, Ganong A, Cotman CW. Long-term potentiation in the hippocampus involves activation in N-methyl-D-aspartate receptors. *Brain Res*. 1984; 323:132–7. [PubMed: 6151863]
49. Morris RGM, Anderson E, Lynch GS, Baudry M. Selective impairment of learning and blockade of long-term potentiation by an N-methyl-D-aspartate receptor antagonist, AP5. *Nature*. 1986; 319:774–6. [PubMed: 2869411]
50. Bashir Z, Alford S, Davies S, Randall A, Collingridge G. Long-term potentiation of NMDA receptor-mediated synaptic transmission in the hippocampus. *Nature*. 1991; 349:156–8. [PubMed: 1846031]
51. Tsien JZ, Huerta PT, Tonegawa S. The essential role of hippocampal CA1 NMDA receptor-dependent synaptic plasticity in spatial memory. *Cell*. 1996; 87:1327–38. [PubMed: 8980238]
52. Vedder LC, Smith CC, Flannigan AE, McMahon LL. Estradiol-induced increase in novel object recognition requires hippocampal NR2B-containing NMDA receptors. *Hippocampus*. 2012 DOI:doi: 10.1002/hipo.22068.
53. Heale V, Harley C. MK-801 and AP5 impair acquisition, but not retention, of the Morris milk maze. *Pharmacol Biochem Behav*. 1990; 36:145–9. [PubMed: 1971949]
54. Alessandri B, Battig K, Welzl H. Effects of ketamine on tunnel maze and water maze performance in the rat. *Behav Neural Biol*. 1989; 52:194–212. [PubMed: 2552977]
55. Morris RG, Anderson E, Lynch GS, Baudry M. Selective impairment of learning and blockade of long-term potentiation by an N-methyl-D-aspartate receptor antagonist, AP5. *Nature*. 1986; 319:774–6. [PubMed: 2869411]
56. Lee H, Kim JJ. Amygdalar NMDA receptors are critical for new fear learning in previously fear-conditioned rats. *J Neurosci*. 1998; 18:8444–54. [PubMed: 9763487]
57. Winters BD, Tucci MC, DaCosta-Furtado M. Older and stronger object memories are selectively destabilized by reactivation in the presence of new information. *Learn Mem*. 2009; 16:545–53. [PubMed: 19713353]
58. Fontan-Lozano A, Saez-Cassanelli JL, Inda MC, de los Santos-Arteaga M, Sierra-Dominguez SA, Lopez-Lluch G, et al. Caloric restriction increases learning consolidation and facilitates synaptic plasticity through mechanisms dependent on NR2B subunits of the NMDA receptor. *J Neurosci*. 2007; 27:10185–95. [PubMed: 17881524]
59. Ge Y, Dong Z, Bagot RC, Howland JG, Phillips AG, Wong TP, et al. Hippocampal long-term depression is required for the consolidation of spatial memory. *Proc Natl Acad Sci U S A*. 2010; 107:16697–702. [PubMed: 20823230]
60. Dong Z, Bai Y, Wu X, Li H, Gong B, Howland JG, et al. Hippocampal long-term depression mediates spatial reversal learning in the Morris water maze. *Neuropharmacology*. 2013; 64:65–73. [PubMed: 22732443]

61. Magnusson KR. Aging of glutamate receptors: correlations between binding and spatial memory performance in mice. *Mech Ageing Dev.* 1998; 104:227–48. [PubMed: 9818728]
62. Magnusson KR. Influence of diet restriction on NMDA receptor subunits and learning during aging. *Neurobiol Aging.* 2001; 22:613–27. [PubMed: 11445262]
63. Magnusson KR, Kresge D, Supon J. Differential effects of aging on NMDA receptors in the intermediate versus the dorsal hippocampus. *Neurobiol Aging.* 2006; 27:324–33. [PubMed: 16399215]
64. Ontl T, Xing Y, Bai L, Kennedy E, Nelson S, Wakeman M, et al. Development and aging of N-methyl-D-aspartate receptor expression in the prefrontal/frontal cortex of mice. *Neuroscience.* 2004; 123:467–79. [PubMed: 14698754]
65. Magnusson KR. Declines in mRNA expression of different subunits may account for differential effects of aging on agonist and antagonist binding to the NMDA receptor. *J Neurosci.* 2000; 20:1666–74. [PubMed: 10684868]
66. Wenk GL, Walker LC, Price DL, Cork LC. Loss of NMDA, but not GABA-A, binding in the brains of aged rats and monkeys. *Neurobiol Aging.* 1991; 12:93–8. [PubMed: 1646968]
67. Das SR, Magnusson KR. Relationship between mRNA expression of splice forms of the zeta1 subunit of the N-methyl-D-aspartate receptor and spatial memory in aged mice. *Brain Res.* 2008; 1207:142–54. [PubMed: 18374315]
68. Magnusson KR. Differential effects of aging on binding sites of the activated NMDA receptor complex in mice. *Mech Ageing Dev.* 1995; 84:227–43. [PubMed: 8788777]
69. Magnusson KR. Influence of dietary restriction on ionotropic glutamate receptors during aging in C57B1 mice. *Mech Ageing Dev.* 1997; 95:187–202. [PubMed: 9179830]
70. Magnusson KR, Cotman CW. Effects of aging on NMDA and MK801 binding sites in mice. *Brain Res.* 1993; 604:334–7. [PubMed: 8457861]
71. Magnusson KR, Cotman CW. Age-related changes in excitatory amino acid receptors in two mouse strains. *Neurobiol Aging.* 1993; 14:197–206. [PubMed: 8391661]
72. Kito S, Miyoshi R, Nomoto T. Influence of age on NMDA receptor complex in rat brain studied by in vitro autoradiography. *J Histochem Cytochem.* 1990; 38:1725–31. [PubMed: 2147708]
73. Piggott MA, Perry EK, Perry RH, Court JA. [³H]MK-801 binding to the NMDA receptor complex, and its modulation in human frontal cortex during development and aging. *Brain Res.* 1992; 588:277–86. [PubMed: 1393579]
74. Gallagher M, Nicolle MM. Animal models of normal aging: Relationship between cognitive decline and markers in hippocampal circuitry. *Behav Brain Res.* 1993; 57:155–62. [PubMed: 7906946]
75. Rapp P, Rosenberg R, Gallagher M. An evaluation of spatial information processing in aged rats. *Behav Neurosci.* 1987; 101:3–12. [PubMed: 3828055]
76. Gage FH, Dunnett SB, Bjorklund A. Spatial learning and motor deficits in aged rats. *Neurobiol Aging.* 1984; 5:43–8. [PubMed: 6738785]
77. Davis S, Markowska AL, Wenk GL, Barnes CA. Acetyl-L-carnitine: behavioral, electrophysiological, and neurochemical effects. *Neurobiol Aging.* 1993; 14:107–15. [PubMed: 8095700]
78. Das SR, Magnusson KR. Changes in expression of splice cassettes of NMDA receptor GluN1 subunits within the frontal lobe and memory in mice during aging. *Behav Brain Res.* 2011; 222:122–33. [PubMed: 21443909]
79. Dingledine R, Borges K, Bowie D, Traynelis SF. The glutamate receptor ion channels. *Pharmacol Rev.* 1999; 51:7–61. [PubMed: 10049997]
80. Collingridge GL, Olsen RW, Peters J, Spedding M. A nomenclature for ligand-gated ion channels. *Neuropharmacology.* 2009; 56:2–5. [PubMed: 18655795]
81. Clayton DA, Browning MD. Deficits in the expression of the NR2B subunit in the hippocampus of aged Fisher 344 rats. *Neurobiol Aging.* 2001; 22:165–8. [PubMed: 11164294]
82. Bai L, Hof PR, Standaert DG, Xing Y, Nelson SE, Young AB, et al. Changes in the expression of the NR2B subunit during aging in macaque monkeys. *Neurobiol Aging.* 2004; 25:201–8. [PubMed: 14749138]

83. Magnusson KR, Nelson SE, Young AB. Age-related changes in the protein expression of subunits of the NMDA receptor. *Brain Res Mol Brain Res*. 2002; 99:40–5. [PubMed: 11869807]
84. Kuehl-Kovarik MC, Magnusson KR, Premkumar LS, Partin KM. Electrophysiological analysis of NMDA receptor subunit changes in the aging mouse cortex. *Mech Ageing Dev*. 2000; 115:39–59. [PubMed: 10854628]
85. Kuehl-Kovarik MC, Partin KM, Magnusson KR. Acute dissociation for analyses of NMDA receptor function in cortical neurons during aging. *J Neurosci Methods*. 2003; 129:11–7. [PubMed: 12951228]
86. Clayton DA, Mesches MH, Alvarez E, Bickford PC, Browning MD. A hippocampal NR2B deficit can mimic age-related changes in long-term potentiation and spatial learning in the Fischer 344 rat. *J Neurosci*. 2002; 22:3628–37. [PubMed: 11978838]
87. Tang YP, Shimizu E, Dube GR, Rampon C, Kerchner GA, Zhuo M, et al. Genetic enhancement of learning and memory in mice. *Nature*. 1999; 401:63–9. [PubMed: 10485705]
88. Cao X, Cui Z, Feng R, Tang YP, Qin Z, Mei B, et al. Maintenance of superior learning and memory function in NR2B transgenic mice during ageing. *Eur J Neurosci*. 2007; 25:1815–22. [PubMed: 17432968]
89. Benitez JA, Segovia J. Gene therapy targeting in the central nervous system. *Curr Gene Ther*. 2003; 3:127–45. [PubMed: 12653406]
90. Berkner KL. Expression of heterologous sequences in adenoviral vectors. *Curr Top Microbiol Immunol*. 1992; 158:39–66. [PubMed: 1582245]
91. Dong JY, Fan PD, Frizzell RA. Quantitative analysis of the packaging capacity of recombinant adeno-associated virus. *Hum Gene Ther*. 1996; 7:2101–12. [PubMed: 8934224]
92. Mizuguchi H, Xu Z, Ishii-Watabe A, Uchida E, Hayakawa T. IRES-dependent second gene expression is significantly lower than cap-dependent first gene expression in a bicistronic vector. *Mol Ther*. 2000; 1:376–82. [PubMed: 10933956]
93. Thomas CE, Ehrhardt A, Kay MA. Progress and problems with the use of viral vectors for gene therapy. *Nat Rev Genet*. 2003; 4:346–58. [PubMed: 12728277]
94. Byrnes AP, Rusby JE, Wood MJ, Charlton HM. Adenovirus gene transfer causes inflammation in the brain. *Neuroscience*. 1995; 66:1015–24. [PubMed: 7651606]
95. Das SR, Jensen R, Kelsay R, Shumaker M, Bochart R, Brim B, et al. Reducing expression of GluN1(OXX) subunit splice variants of the NMDA receptor interferes with spatial reference memory. *Behav Brain Res*. 2012; 230:317–24. [PubMed: 22360858]
96. Charizanis K, Lee KY, Batra R, Goodwin M, Zhang C, Yuan Y, et al. Muscleblind-like 2-mediated alternative splicing in the developing brain and dysregulation in myotonic dystrophy. *Neuron*. 2012; 75:437–50. [PubMed: 22884328]
97. Foster TC, Rani A, Kumar A, Cui L, Semple-Rowland SL. Viral vector-mediated delivery of estrogen receptor-alpha to the hippocampus improves spatial learning in estrogen receptor-alpha knockout mice. *Mol Ther*. 2008; 16:1587–93. [PubMed: 18594506]
98. Foster TC, Kumar A. Susceptibility to induction of long-term depression is associated with impaired memory in aged Fischer 344 rats. *Neurobiol Learn Mem*. 2007; 87:522–35. [PubMed: 17276704]
99. Kumar A. Carbachol-induced long-term synaptic depression is enhanced during senescence at hippocampal CA3-CA1 synapses. *J Neurophysiol*. 2010; 104:607–16. [PubMed: 20505129]
100. Kumar A, Foster TC. 17beta-Estradiol benzoate decreases the AHP amplitude in CA1 pyramidal neurons. *J Neurophysiol*. 2002; 88:621–6. [PubMed: 12163515]
101. Kumar A, Foster TC. Enhanced long-term potentiation during aging is masked by processes involving intracellular calcium stores. *J Neurophysiol*. 2004; 91:2437–44. [PubMed: 14762159]
102. Kumar A, Foster TC. Intracellular calcium stores contribute to increased susceptibility to LTD induction during aging. *Brain Res*. 2005; 1031:125–8. [PubMed: 15621020]
103. Kumar A, Foster TC. Shift in induction mechanisms underlies an age-dependent increase in DHPG-induced synaptic depression at CA3 CA1 synapses. *J Neurophysiol*. 2007; 98:2729–36. [PubMed: 17898145]

104. Kumar A, Thinschmidt JS, Foster TC, King MA. Aging effects on the limits and stability of long-term synaptic potentiation and depression in rat hippocampal area CA1. *J Neurophysiol.* 2007; 98:594–601. [PubMed: 17553951]
105. Kumar A, Rani A, Tchigranova O, Lee WH, Foster TC. Influence of late-life exposure to environmental enrichment or exercise on hippocampal function and CA1 senescent physiology. *Neurobiol Aging.* 2012; 33:828, e1–e17. [PubMed: 21820213]
106. Bodhinathan K, Kumar A, Foster TC. Intracellular redox state alters NMDA receptor response during aging through Ca²⁺/Calmodulin-dependent protein kinase II. *J Neurosci.* 2010; 30:1914–24. [PubMed: 20130200]
107. Streit WJ. An improved staining method for rat microglial cells using the lectin from *Griffonia simplicifolia* (GSA I-B4). *J Histochem Cytochem.* 1990; 38:1683–6. [PubMed: 2212623]
108. Fischer G, Mutel V, Trube G, Malherbe P, Kew JN, Mohacs E, et al. Ro 25-6981, a highly potent and selective blocker of N-methyl-D-aspartate receptors containing the NR2B subunit. Characterization in vitro. *J Pharmacol Exp Ther.* 1997; 283:1285–92. [PubMed: 9400004]
109. Cui Y, Jin J, Zhang X, Xu H, Yang L, Du D, et al. Forebrain NR2B overexpression facilitating the prefrontal cortex long-term potentiation and enhancing working memory function in mice. *PLoS One.* 2011; 6:e20312. [PubMed: 21655294]
110. Zhang X, Nadler JV. Postsynaptic response to stimulation of the Schaffer collaterals with properties similar to those of synaptosomal aspartate release. *Brain Res.* 2009; 1295:13–20. [PubMed: 19664606]
111. Wang D, Cui Z, Zeng Q, Kuang H, Wang LP, Tsien JZ, et al. Genetic enhancement of memory and long-term potentiation but not CA1 long-term depression in NR2B transgenic rats. *PLoS One.* 2009; 4:e7486. [PubMed: 19838302]
112. Foster KA, McLaughlin N, Edbauer D, Phillips M, Bolton A, Constantine-Paton M, et al. Distinct roles of NR2A and NR2B cytoplasmic tails in long-term potentiation. *J Neurosci.* 2010; 30:2676–85. [PubMed: 20164351]
113. Howland JG, Cazakoff BN. Effects of acute stress and GluN2B-containing NMDA receptor antagonism on object and object-place recognition memory. *Neurobiol Learn Mem.* 2010; 93:261–7. [PubMed: 19857581]
114. Higgins GA, Ballard TM, Huwyler J, Kemp JA, Gill R. Evaluation of the NR2B-selective NMDA receptor antagonist Ro 63-1908 on rodent behaviour: evidence for an involvement of NR2B NMDA receptors in response inhibition. *Neuropharmacology.* 2003; 44:324–41. [PubMed: 12604092]
115. Colucci M, Maione F, Bonito MC, Piscopo A, Di Giannuario A, Pieretti S. New insights of dimethyl sulphoxide effects (DMSO) on experimental in vivo models of nociception and inflammation. *Pharmacol Res.* 2008; 57:419–25. [PubMed: 18508278]
116. Wei F, Wang GD, Kerchner GA, Kim SJ, Xu HM, Chen ZF, et al. Genetic enhancement of inflammatory pain by forebrain NR2B overexpression. *Nat Neurosci.* 2001; 4:164–9. [PubMed: 11175877]
117. Morris, RGM.; Davis, M. The role of NMDA receptors in learning and memory. In: Collingridge, GL.; Watkins, JC., editors. *The NMDA Receptor.* Oxford: Oxford University Press; 1994. p. 340-75.
118. Lattal KM, Abel T. Different requirements for protein synthesis in acquisition and extinction of spatial preferences and context-evoked fear. *J Neurosci.* 2001; 21:5773–80. [PubMed: 11466449]
119. Bourchouladze R, Abel T, Berman N, Gordon R, Lapidus K, Kandel ER. Different training procedures recruit either one or two critical periods for contextual memory consolidation, each of which requires protein synthesis and PKA. *Learn Mem.* 1998; 5:365–74. [PubMed: 10454361]
120. Liang KC, Hon W, Tyan YM, Liao WL. Involvement of hippocampal NMDA and AMPA receptors in acquisition, formation and retrieval of spatial memory in the Morris water maze. *Chin J Physiol.* 1994; 37:201–12. [PubMed: 7796636]
121. Vafaei AA, Rashidy-Pour A. Reversible lesion of the rat's orbitofrontal cortex interferes with hippocampus-dependent spatial memory. *Behav Brain Res.* 2004; 149:61–8. [PubMed: 14739010]

122. Hall BJ, Ripley B, Ghosh A. NR2B signaling regulates the development of synaptic AMPA receptor current. *J Neurosci.* 2007; 27:13446–56. [PubMed: 18057203]
123. Akashi K, Kakizaki T, Kamiya H, Fukaya M, Yamasaki M, Abe M, et al. NMDA receptor GluN2B (GluR epsilon 2/NR2B) subunit is crucial for channel function, postsynaptic macromolecular organization, and actin cytoskeleton at hippocampal CA3 synapses. *J Neurosci.* 2009; 29:10869–82. [PubMed: 19726645]
124. Zhao MG, Toyoda H, Lee YS, Wu LJ, Ko SW, Zhang XH, et al. Roles of NMDA NR2B subtype receptor in prefrontal long-term potentiation and contextual fear memory. *Neuron.* 2005; 47:859–72. [PubMed: 16157280]
125. Brigman JL, Wright T, Talani G, Prasad-Mulcare S, Jinde S, Seabold GK, et al. Loss of GluN2B-containing NMDA receptors in CA1 hippocampus and cortex impairs long-term depression, reduces dendritic spine density, and disrupts learning. *J Neurosci.* 2010; 30:4590–600. [PubMed: 20357110]
126. Watson DJ, Stanton ME. Intrahippocampal administration of an NMDA-receptor antagonist impairs spatial discrimination reversal learning in weanling rats. *Neurobiol Learn Mem.* 2009; 92:89–98. [PubMed: 19248837]
127. Duffy S, Labrie V, Roder JC. D-serine augments NMDA-NR2B receptor-dependent hippocampal long-term depression and spatial reversal learning. *Neuropsychopharmacology.* 2008; 33:1004–18. [PubMed: 17625504]
128. Horst NK, Laubach M. The role of rat dorsomedial prefrontal cortex in spatial working memory. *Neuroscience.* 2009; 164:444–56. [PubMed: 19665526]
129. Wong RW, Setou M, Teng J, Takei Y, Hirokawa N. Overexpression of motor protein KIF17 enhances spatial and working memory in transgenic mice. *Proc Natl Acad Sci U S A.* 2002; 99:14500–5. [PubMed: 12391294]
130. Paxinos, G.; Franklin, KBJ. *The Mouse Brain atlas.* 2. San Deigo, CA: Academic Press; 2007.

Highlights

- Enhanced GluN2B expression improves memory in aged animals, similar to young.
- Enhanced GluN2B expression in the frontal cortex improves later long-term memory.
- Enhanced GluN2B expression in the hippocampus improves early long-term memory.
- Enhanced GluN2B expression increases NMDA receptor-mediated synaptic transmission.
- Enhancement of GluN2B expression in the aged brain may have therapeutic potential.
- Future studies will elucidate how enhanced GluN2B expression is being beneficial for memory.

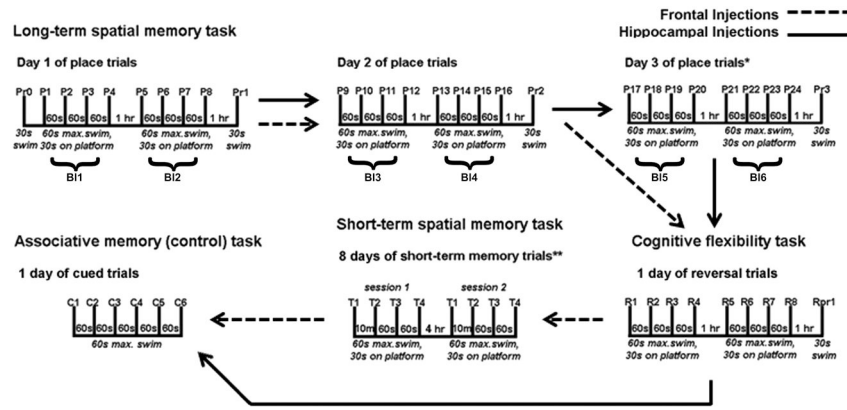


Fig. 1. Schematic of the various memory tasks used to assess memory in the Morris water maze. Tasks used include the spatial long-term memory task, the spatial delayed short-term memory task, the cognitive flexibility task and the associative memory (control) task. *Only mice that received hippocampal injections had a 3rd day of spatial long-term memory testing. **Only mice that received the frontal lobe injections were characterized in the spatial delayed short-term memory task. s= seconds; m= minutes; hr= hour; max= maximum time; Pr= probe trial; P= place trial; R= reversal trial; T= short-term memory trial; C= cued trial; Bl= block of 4 place trials.

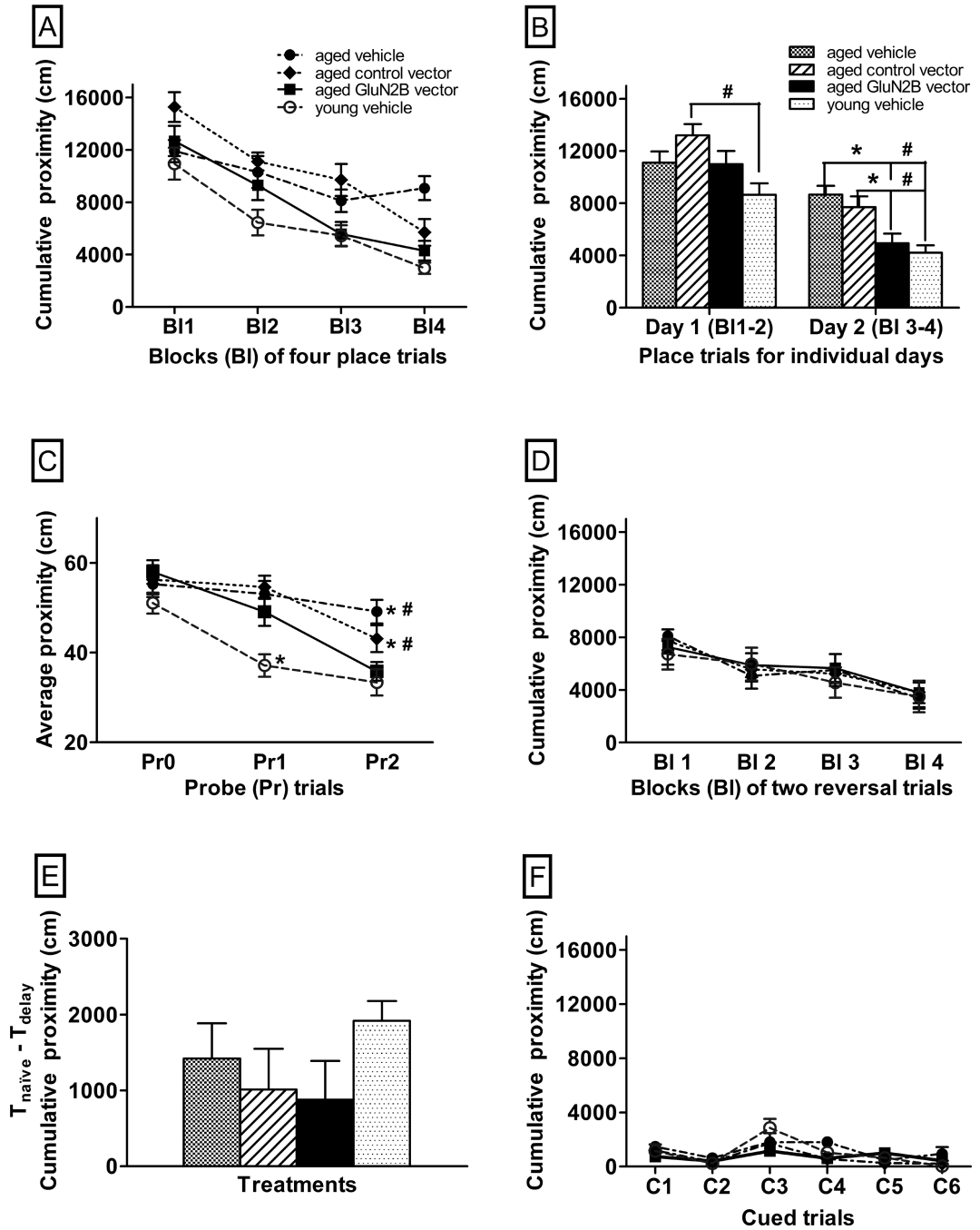


Fig. 2. The effects of enhanced GluN2B expression in the frontal lobe on the performance of aged mice in memory tasks in the Morris water maze. Graphs A–F show the effects of the GluN2B vector or 2 control (control vector or vehicle) treatments on learning performance. In graphs A–D and F, lower proximity scores represent better performance. In graph E, greater differences between naïve and delayed trials represent better performance. The performance of young vehicle-treated mice is included for comparison. (A) Performance across blocks of four place trials for the two-day long-term spatial memory task. (B) Performance averaged across place trials for each individual day of the two-day long-term spatial memory task. (C) Performance within probe trials of the two-day long-term spatial

memory task. (D) Performance across blocks of two reversal trials for the flexibility task. (E) Differences in performance between $T_{\text{naïve}}$ and T_{delay} trials, averaged over delayed short-term spatial memory sessions, over eight days. (F) Performance in 6 cued trials for the associative memory task. * p 0.05 for differences from aged GluN2B vector-treated mice and # p 0.05 for differences from young vehicle-treated mice as determined by repeated measures and two-way ANOVA, followed by Fisher's protected least significant difference post-hoc analysis. N=12–14. Bl = block of 4 place trials, Pr = probe trials, Pr0= naïve probe trials, R= reversal trials, C= cued trials. Error bars = standard error of the mean (SEM).

\$watermark-text

\$watermark-text

\$watermark-text

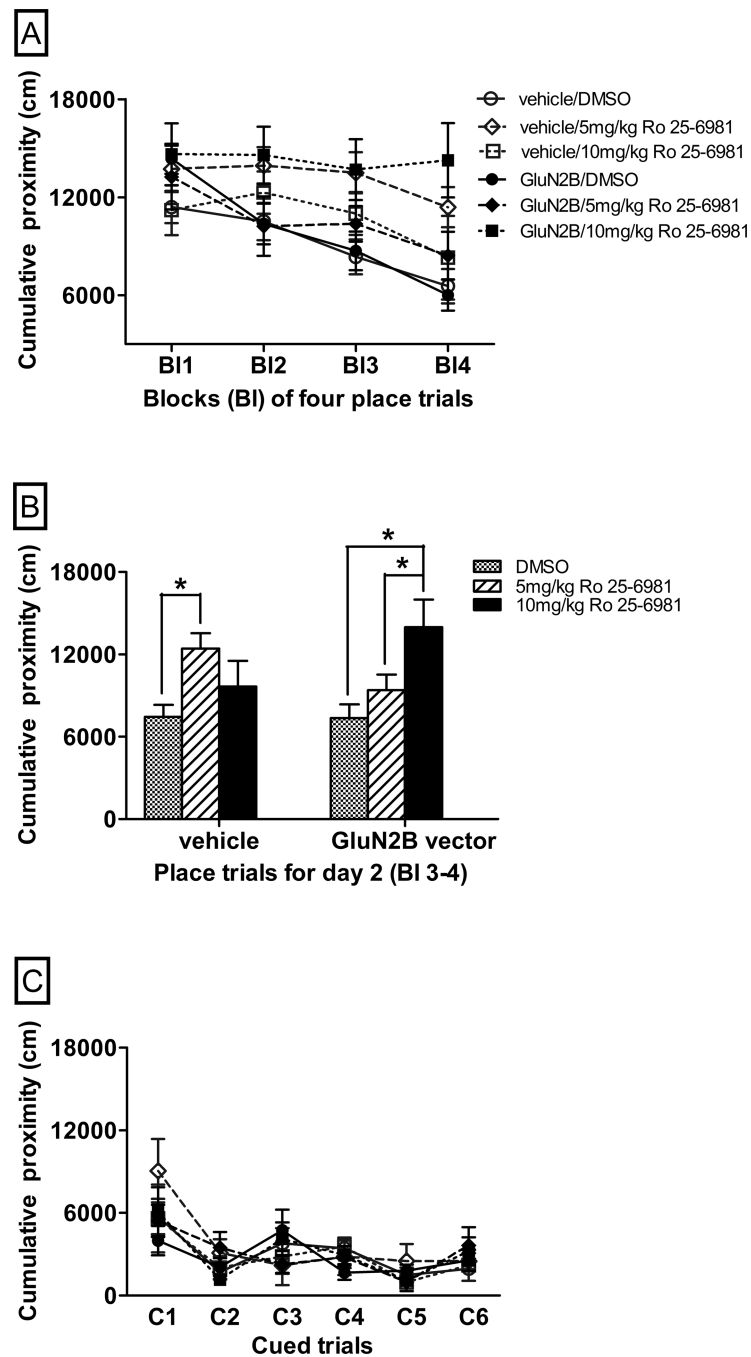


Fig. 3. The effects of the GluN2B antagonist, Ro 25-6981, on the performance of aged mice with enhanced GluN2B expression in two memory tasks in the Morris water maze. Graphs A–C show the effects of Ro 25-6981 antagonism on the performance of aged mice receiving frontal lobe injections of GluN2B vector or vehicle, with lower proximity scores representing better performance. (A) Learning performance of aged mice across blocks of place trials for the two-day long-term spatial memory task. (B) Learning performance of aged mice averaged across place trials for day 2 of the two-day long-term spatial memory task. (C) Performance of aged mice in 6 cued trials for the associative memory task. * $p < 0.05$ for differences in performance between treatment groups indicated as determined by

repeated measures and two-way ANOVA, followed by Fisher's protected least significant difference post-hoc analysis. N=4-16. B1 = blocks of 4 place trials, C= cued trials. Error bars = standard error of the mean (SEM).

\$watermark-text

\$watermark-text

\$watermark-text

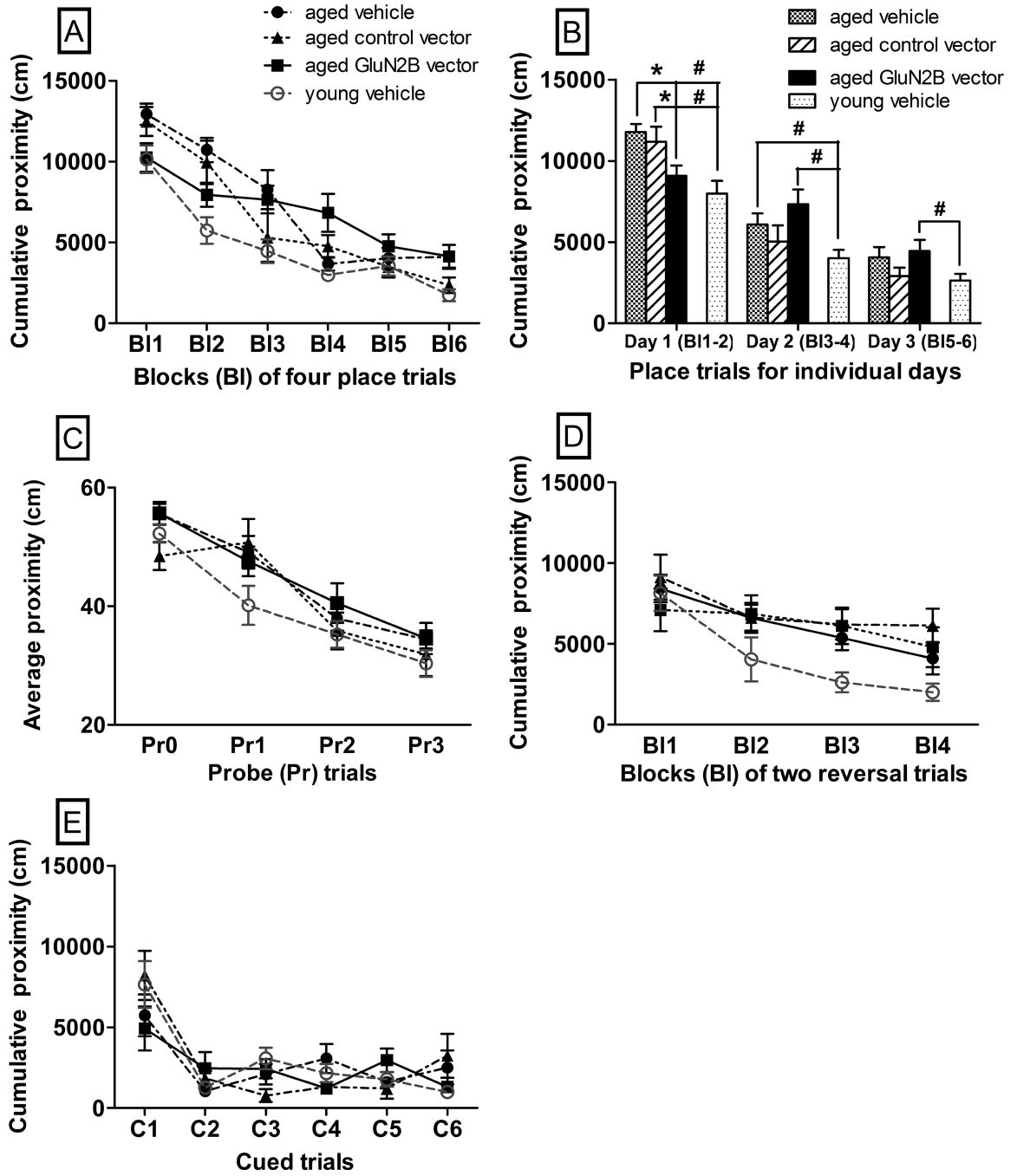


Fig. 4. The effects of enhanced GluN2B expression in the hippocampus on the performance of aged mice in memory tasks in the Morris water maze. Graphs A–E show the effects of the GluN2B vector or 2 control (control vector or vehicle) treatments on learning performance. In graphs A–E, lower proximity scores represent better performance. (A) Performance within blocks of four place trials for the three-day long-term spatial memory task. (B) Performance averaged across place trials for individual days for the three-day long-term spatial memory task. (C) Performance within probe trials of the three-day long-term spatial memory task. (D) Performance across blocks of two reversal trials for the flexibility task. (E) Performance in 6 cued trials for the associative memory task. * $p < 0.05$ for differences

from aged GluN2B vector-treated mice and # $p < 0.05$ for differences from young vehicle-treated mice as determined by repeated measures and two-way ANOVA followed by Fisher's protected least significant difference post-hoc analysis. N=7–15. Bl = blocks of 4 place trials or 2 reversal trials, Pr = probe trials, Pr0= naïve probe trials, C= cued trials. Error bars = standard error of the mean (SEM).

\$watermark-text

\$watermark-text

\$watermark-text

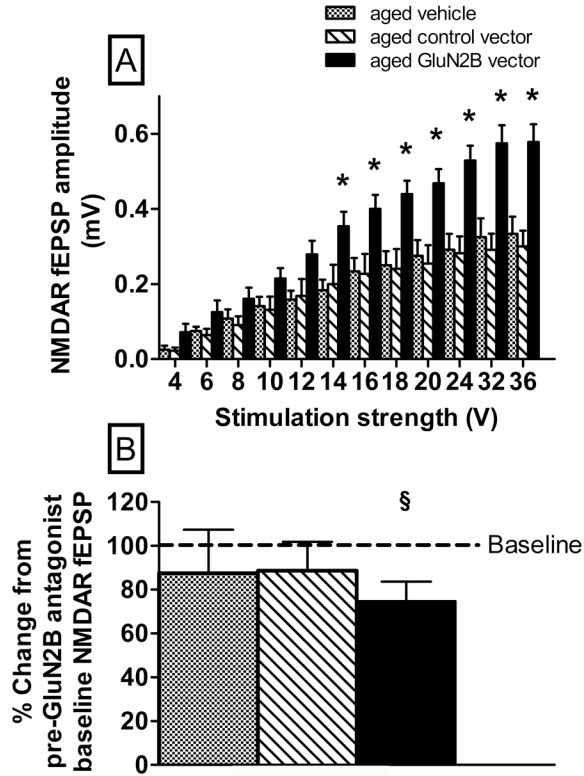


Fig. 5. The effects of enhanced GluN2B subunit expression in the hippocampus of aged mice on the NMDA receptor-mediated EPSP responses in hippocampal slices. (A) Input-output curves for the mean NMDA receptor-mediated EPSP amplitude versus stimulus intensity. GluN2B vector treated slices exhibited significant increase in NMDA receptor-mediated EPSP for higher stimulus intensities compared to 2 control (control vector or vehicle) treatments. (B) Percent change in NMDA receptor-mediated EPSP compared to baseline (dotted line) for the last 5 min following 60 min bath application of Ro 25-6981. **p* 0.05 for differences in responses from control vector and vehicle treatment groups determined by (A) Fisher’s protected least significant difference between GluN2B and controls for each intensity or §*p* 0.05 for differences in response from baseline (B) one sample t-test. N=3–14. Error bars =standard error of the mean (SEM).

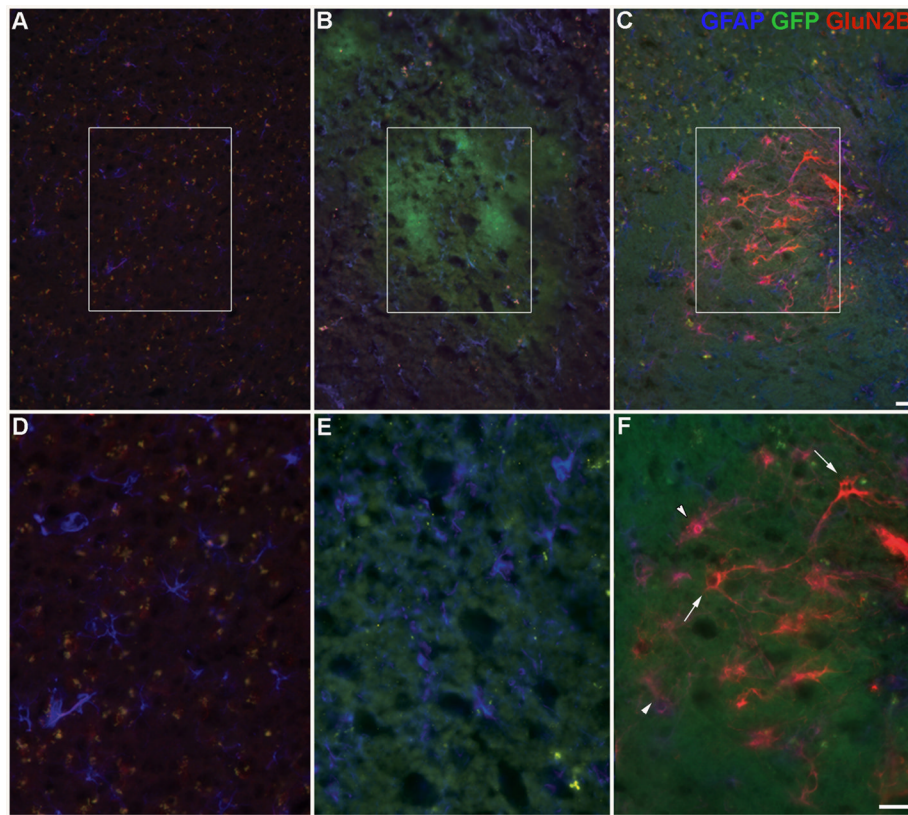


Fig. 6. Enhanced GluN2B subunit expression *in vivo* in the frontal lobe. Representative images of coronal sections showing GluN2B subunit, GFP (vector reporter) and GFAP (glial marker) protein expression within the frontal lobe in different treatments: (A, D) vehicle, (B, E) control vector and (C, F) GluN2B vector within aged mice. Panels D–F are higher magnification images of areas shown in panels A–C, respectively. Green= GFP (*in vivo*), Red= GluN2B subunit, Blue= GFAP, Yellow= lipofuscin, co-localized GFP and GluN2B = orange, co-localized GFAP and GluN2B= purple, GluN2B subunit in neuronal-like cells (arrows), GluN2B subunit in astrocytes (arrowheads). Bar= 25 μ m.

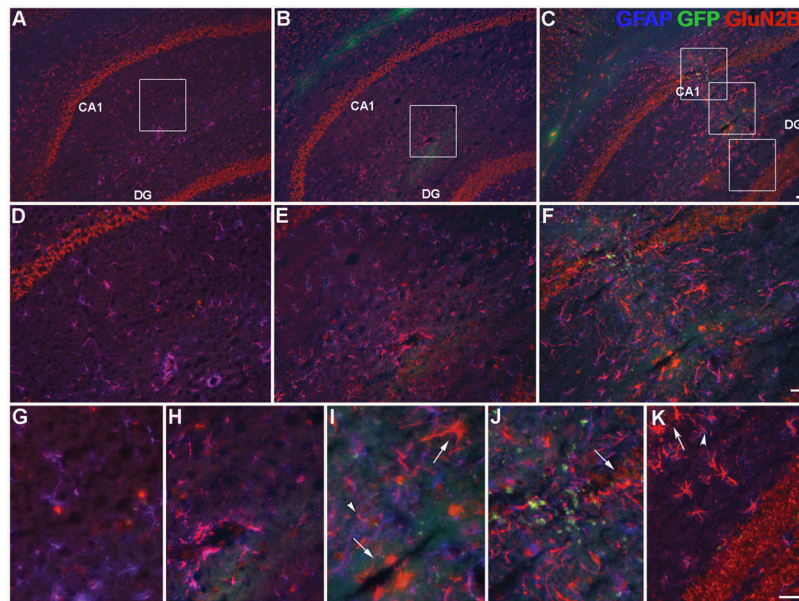


Fig. 7. Enhanced GluN2B subunit expression *in vivo* in the hippocampus. Representative images of coronal sections showing GluN2B subunit, GFP (vector reporter) and GFAP (glial marker) protein expression within the hippocampus in different treatments: (A, D, G) vehicle, (B, E, H) control vector and (C, F, I, J, K) GluN2B vector in aged mice. Panels D–K represent higher magnification images of areas shown in panels A–C, respectively. Green= GFP (*in vivo*), Red= GluN2B subunit, Blue= GFAP, Yellow= lipofuscin, co-localized GFP and GluN2B = orange, co-localized GFAP and GluN2B= purple, GluN2B subunit in neuronal-like cells (arrows), GluN2B subunit in astrocytes (arrowheads). I) CA1 stratum radiatum. J) CA1 stratum pyramidale. K) dentate gyrus molecular layer, upper blade. Bar= 25 μ m.

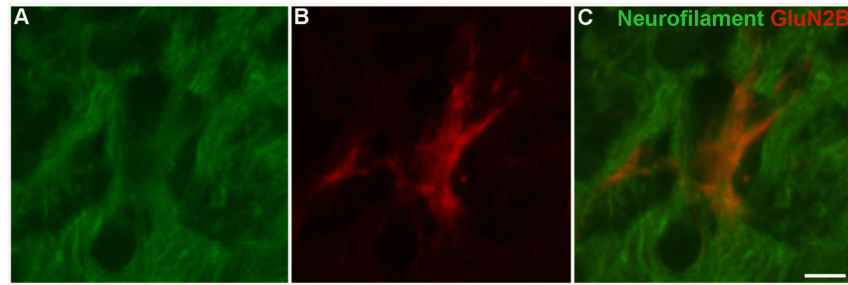


Fig. 8. Enhanced GluN2B subunit expression *in vivo* in neurons. Representative image of a coronal section showing GluN2B subunit and neurofilament (neuronal marker) protein expression within the frontal lobe of an aged mouse treated with GluN2B vector. Panel A shows neurofilament only and Panel B shows GluN2B subunit only. Panel C shows GluN2B subunit with neurofilament. Red= GluN2B subunit, Green= neurofilament, co-localized neurofilament and GluN2B= orange, Bar= 5 μ m.

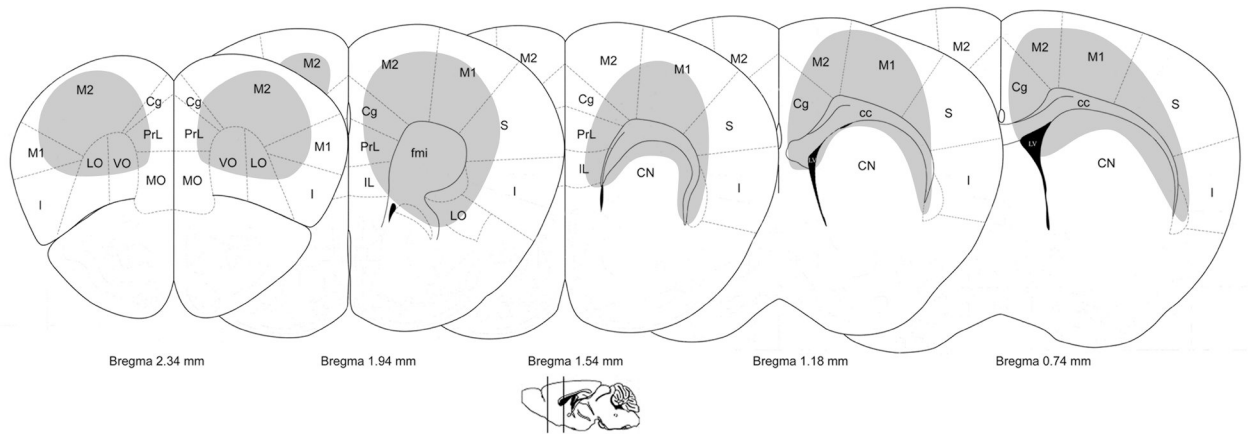


Fig. 9.

Brain regions with enhanced GluN2B expression in the frontal lobe and caudate nucleus. Representative diagrams of coronal sections (adapted from [130]) show the locations of cells that were intensely labeled for the GluN2B subunit across the frontal lobe and caudate nucleus. cc= corpus callosum; Cg= cingulate cortex; CN= caudate nucleus; fmi= forceps minor of the corpus callosum; I= insular cortex; IL= infralimbic cortex; LO= lateral orbital cortex; LV= lateral ventricle; M1= primary motor cortex M2= secondary motor cortex; MO= medial orbital cortex; PrL= prelimbic cortex; S= somatosensory cortex; VO= ventral orbital cortex.

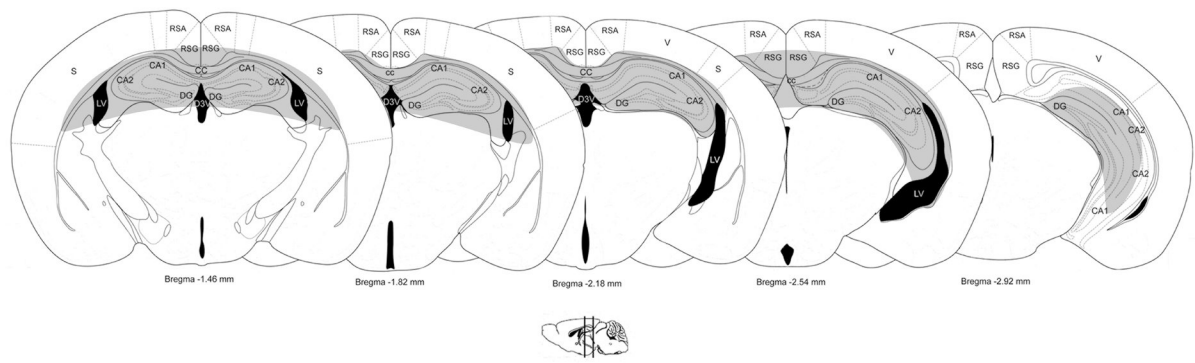


Fig. 10.

Brain regions with enhanced GluN2B expression in the hippocampus. Representative diagrams of coronal sections (adapted from [130]) show the location of cells intensely labeled for the GluN2B subunit across the hippocampus. CA1= *Cornu Ammonis 1*; CA2= *Cornu Ammonis 2*; CA3= *Cornu Ammonis 3*; cc= corpus callosum; D3V= dorsal 3rd ventricle; LV= lateral ventricle; RSA= retrosplenial agranular cortex, RSG= retrosplenial granular cortex; S= somatosensory cortex; V= visual cortex.

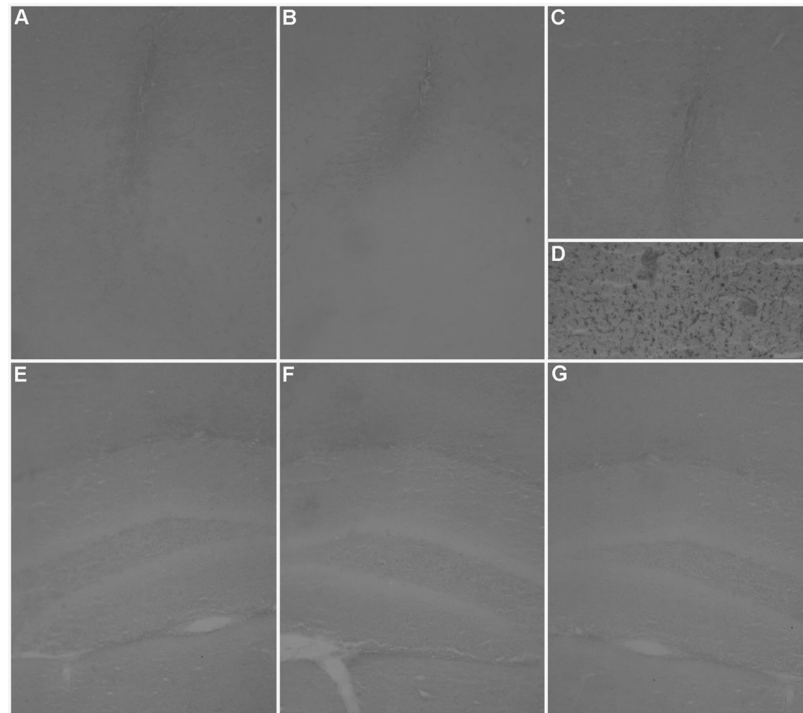


Fig. 11. Inflammation in vector-treated mice was not increased over vehicle-treated mice in the frontal lobe or hippocampus. Panels A–G show isolectin B₄ staining of microglia in representative coronal sections taken at the injection site in the frontal lobe or hippocampus. (D) Inflammation was visible in a lipopolysaccharide-treated brain (positive control) and, to a lesser extent, equally across the different treatments, within the injection sites only: (A, E) vehicle, (B, F) control vector and (C, G) GluN2B vector. Bar=50 μ m.